RECOVERING THE PRIMORDIAL DENSITY FLUCTUATIONS: A COMPARISON OF METHODS

Vijay K. Narayanan and Rupert A.C. Croft

Department of Astronomy, The Ohio State University, Columbus, OH 43210; vijay,racc@astronomy.ohio-state.edu Email: vijay,racc@astronomy.ohio-state.edu

ABSTRACT

We present a comparative study of different methods for reversing the gravitational evolution of a cosmological density field to recover the primordial fluctuations. We test six different approximate schemes in all: linear theory, the Gaussianization technique of Weinberg (1992), two different quasi-linear dynamical schemes (Nusser & Dekel 1992, Gramann 1993), a hybrid dynamical-Gaussianization method (Narayanan & Weinberg 1998) and the Path Interchange Zel'dovich Approximation (PIZA) of Croft & Gaztañaga (1997). The final evolved density field from an N-body simulation constitutes our test case. We use a variety of statistical measures to compare the initial density field recovered from it to the true initial density field, using each of the six different schemes. These include point-by-point comparisons of the density fields in real space, and the individual modes in Fourier space, as well as global statistical properties such as the genus, the PDF of the density, and the distribution of peak heights and their shapes. We find linear theory to be substantially less accurate than the other schemes, all of which reverse at least some of the non-linear effects of gravitational evolution even on scales as small as $3h^{-1}$ Mpc. The Gaussianization scheme, while being robust and easy to apply, is the least accurate after linear theory. The two quasilinear dynamical schemes, which are based on Eulerian formulations of the Zel'dovich Approximation, give similar results to each other and are more accurate than Gaussianization, although they break down quite drastically when used outside their range of validity, the quasilinear regime. The complementary beneficial aspects of the dynamical and the Gaussianization schemes are combined in the Hybrid method, which uses a dynamical scheme to account for the bulk displacements of mass elements and corrects for any systematic errors using Gaussianization. We find this reconstruction scheme to be more accurate and robust than either the Gaussianization or dynamical method alone. The final scheme, the PIZA, performs substantially better than the others in all point by point comparisons. The PIZA does produce an oversmoothed initial density field, with a smaller number of peaks than expected, but recovers the PDF of the initial density with impressive accuracy on scales as small as $3h^{-1}$ Mpc.

Subject headings: cosmology: theory, galaxies: clustering, large scale structure of Universe

1. INTRODUCTION

In the standard model of structure formation, the observed galaxy distribution arises from the growth by gravitational instability of small amplitude primordial density fluctuations. We need to understand the characteristics of these seed density perturbations if we are to trace the history of structure formation in the universe. In the simplest inflationary model for the origin of these perturbations, the primordial density fluctuations on the astrophysically relevant scales arise from the quantum noise in the inflaton field (Guth & Pi 1982; Hawking 1982; Starobinsky 1982; Bardeen, Steinhardt, & Turner 1983). Another class of models identifies these seed fluctuations with the topological defects that remain as the relics of high energy phase transitions (Kibble 1976). We need to confront all these models with observational data to decide which model, if any, can correctly predict the structure we observe. Such a comparison is non-trivial because, while the theories predict the properties of the primordial fluctuations, the observations measure the properties of the present day density field. Thus, the observed properties reflect the primordial properties after they have been distorted by the non-linear gravitational instability process. The conventional study of the structure formation process has focused on a rather indirect method. In this usual approach, we gravitationally evolve a model for the initial density field forward in time using N-body methods. We then compare the properties of the resulting mass distribution with those of the observed galaxy distribution assuming either that galaxies trace mass or by using a specific plausible biasing prescription to select galaxies. We can then either accept or reject the model of the initial density field depending on how accurately the properties of the simulated galaxy distribution match the observations (Davis et al. 1985). This method requires that we densely explore the full parameter space of all the possible models for the initial density field, and therefore, its applicability is limited both by the accuracy of our comparisons and by the amount of computational time. Under these circumstances, it would be extremely useful if we could reverse the effects of the gravitational evolution and recover the primordial density fluctuations directly from the observed galaxy distribution, as we could then directly analyze its properties. In this paper, we compare the accuracy of the different methods that have been proposed to reverse the effects of gravitational clumping and recover the primordial density fluctuations.

The time evolution of the mass density fluctuations in an expanding background universe is described by a second order differential equation that has both growing and decaying mode solutions (Peebles 1980). A direct numerical integration of this differential equation backwards in time will fail because the decaying mode will amplify any residual noise that is present in the final density field. Therefore, any method for recovering the initial density fluctuations must solve this problem using some approximations regarding the growth of fluctuations or some plausible assumptions about the nature of the initial density fluctuations. In this paper, we classify the various reconstruction schemes that have been proposed into three major categories depending on how they overcome this problem and reverse the effects of gravitational instability. The schemes in the first category are "gravitational time machines" that attempt to run gravity backwards in time. They treat the mass density field as a self gravitating pressureless fluid of particles and solve the

fluid mass and/or momentum conservation equations using a Lagrangian approximation for the particle trajectories. The simplest methods in this scheme assume that the comoving trajectories of the particles are straight lines during gravitational evolution (the Zel'dovich approximation, Zel'dovich 1970). This is a reasonable first approximation because, in linear perturbation theory, the direction of the gravitational acceleration stays constant in time. The Zel'dovich-Bernoulli equation, derived by Nusser & Dekel (1992) from the Euler momentum conservation equation, and the Zel'dovich-continuity equation derived by Gramann (1993) from the mass continuity equation (see also Nusser et al. 1991) fall in this category. These two dynamical schemes describe the time evolution of the velocity potential and the gravitational potential respectively, using first order differential equations that have only growing mode solutions. These equations can then be integrated backwards in time quite easily to recover the corresponding initial potential fields. The initial density field follows from these potential fields from the relevant linear theory relations between these quantities, which we will describe in more detail in §2. Kolatt et al. (1996) used a modified version of the Zel'dovich-Bernoulli scheme to construct mock redshift catalogs of our cosmic neighborhood, which can then be used to study the different biases and selection effects that complicate the analysis of galaxy redshift and peculiar velocity surveys.

The Gaussianization mapping method of Weinberg (1992, hereafter W92) belongs to the second category of reconstruction methods. It is based on the approximation that the rank order of the initial mass density field, smoothed over scales of a few Mpc, is preserved under non-linear gravitational evolution. It further assumes that the initial density fluctuations form a Gaussian random field. The method employs a monotonic mapping of the smoothed final density field to a smoothed initial mass density field that has a Gaussian one-point probability distribution function (PDF). This method was used by Weinberg (1989) to show that a structure as massive as the Perseus-Pisces supercluster (Haynes & Giovanelli 1986) can form from the gravitational instability of small amplitude Gaussian initial density fluctuations. Although in this paper we explicitly assume a Gaussian form for the PDF, this category of reconstruction methods would also naturally include any other schemes which assume a purely local monotonic mapping between the final and initial densities. Using the predicted evolution of the PDF under gravitational instability (with, for example, the Local Lagrangian Approximation of Protogeros & Scherrer [1997] or the Spherical Collapse Model of Fosalba & Gaztañaga [1997]), we can also explore the reconstruction of non-Gaussian initial conditions.

Narayanan & Weinberg (1998, hereafter NW98) proposed a hybrid reconstruction scheme that combines the features of the two categories described above. This method also assumes that the initial density fluctuation field is a Gaussian random field. As shown by NW98, this reconstruction scheme can recover the initial density field more accurately than either the Lagrangian dynamical schemes of the first category or the Eulerian Gaussian mapping scheme of the second category, provided that the true initial density field is indeed a Gaussian random field.

The third category of methods, pioneered by Peebles (1989, 1990), treats the gravitational instability problem as a two-point boundary value problem and solves for the trajectories of

the mass particles by minimizing the action integral. Shaya, Peebles & Tully (1995) used this technique to reconstruct the trajectories and the initial positions of the galaxies within 3000 kms⁻¹ assuming that they started out with vanishingly small initial peculiar velocities. This method is computationally intensive, and so far it has not been applied to the reconstruction of the initial density field over a cosmologically interesting volume. Croft & Gaztañaga (1997, hereafter CG97) demonstrated that the Zel'dovich Approximation is the least action solution when the particle trajectories are approximated by rectilinear paths. This simplifying assumption (which sacrifices some of the potential accuracy of the least action approach) was used by CG97 as the basis for the Path Interchange Zel'dovich Approximation (PIZA) reconstruction method. In this method, the reconstruction problem reduces to finding the straight line trajectories of all particles by satisfying the condition that the total mean square particle displacement between the initial and final positions be a minimum.

In this paper, we test six different reconstruction schemes that fall under these three categories, with a view to check which of these methods can accurately and robustly recover the initial density fluctuation field. The various schemes that we test are: (1) Linear theory, (2) the Zel'dovich-Bernoulli scheme, (3) the Zel'dovich-continuity scheme, (4) Gaussianization, (5) the Hybrid method, and (6) the PIZA scheme. We first gravitationally evolve a known initial density fluctuation field using an N-body simulation code. We assume that the initial fluctuations form a Gaussian random field, as predicted by the simplest inflationary models. This Gaussian assumption is the simplest one among a wide class of assumptions, and there is observational evidence from both microwave background anisotropies (e.g., Kogut et al. 1996; Heavens 1998) and galaxy clustering (e.g., Weinberg, Gott & Melott 1987; Nusser, Dekel & Yahil 1995; Chiu, Ostriker & Strauss 1998) that the primordial mass density fluctuations form a Gaussian random field. We recover the initial density field from the final, non-linear, gravitationally evolved field, using all six of the reconstruction methods listed above. We then use a variety of statistical measures to compare the local and the global properties of the true initial density field with those of the initial density fields recovered by the different reconstruction methods. We examine both point-by-point comparisons between the true and the recovered initial density fields and the ability of the reconstruction methods to accurately recover the Gaussian nature of the initial density field. These comparisons will enable us to understand the relative performance of these reconstruction methods and will be useful for the reconstruction of the primordial fluctuation field from the density field traced by redshift surveys.

All the reconstruction schemes in the first and the second category are designed to derive the initial mass density field from a continuous final density field. Moreover, since the schemes in the first category are based on the perturbation theory expansions of the density and velocity fields, they break down in the strongly non-linear regions (characterized by $|\delta| \gg 1$). Therefore, in all these reconstruction schemes, we reconstruct the smoothed initial density field from a final density field that is smoothed with a Gaussian filter, so that the resulting smoothed final density field does not have any strong non-linearities. On the other hand, the PIZA scheme recovers the

initial density field starting from the final locations of all the mass particles. Thus, in the PIZA scheme alone, we smooth the density field *after* recovering the initial density field.

All the reconstruction schemes require the final mass density distribution, while it is the galaxy distribution that is the observable quantity. In the case of biased galaxy formation, the observed galaxy number density fluctuations are not equal to the underlying mass density fluctuations. Of all these six schemes, the Gaussianization and the hybrid reconstruction schemes can be adapted to reconstruct from biased galaxy density fields in a straightforward manner (see W92 and NW98), on the assumption that the biasing is local, while the other schemes cannot be adapted so easily. However, in this paper, we ignore the possibility of biased galaxy formation and focus purely on gravitational dynamics. In this sense, our work is similar in spirit to the work of Coles et al. (1993) and Sathyaprakash et al. (1995), who compared the validity of different approximations for the forward evolution of a density field under gravitational instability. We note here that we will only test those methods that reconstruct the initial density field from the final density field. We will not test those techniques that use the final peculiar velocity field (e.g., Nusser & Dekel 1992) as the input.

The outline of the paper is as follows. We describe the various reconstruction schemes in detail in §2, and in §3 we describe our test case, the density field from the output of an N-body simulation. In §4, we describe the statistical properties of the six reconstructed density fields and compare them with those of the true initial density field. We then discuss the performance of each of the reconstruction schemes and compare their relative advantages and shortcomings in §5. We also describe the potential problems that might be encountered during an actual reconstruction of the initial mass density fluctuations from present day galaxy redshift catalogs.

2. RECONSTRUCTION SCHEMES

The reconstruction schemes in the first category solve for the time evolution of the density field using perturbation theory expansions of the density and velocity fields. The growth of density contrasts, $\delta(\mathbf{x}) \equiv \left[\rho(\mathbf{x}) - \bar{\rho}\right]/\bar{\rho}$, in an expanding universe can be analyzed using the equations of ideal fluid flow as long as the trajectories of individual fluid elements do not cross (i.e, before any shell crossing). Denoting the comoving distance by \mathbf{x} , the peculiar velocity by $\mathbf{v} = d\mathbf{x}/dD$, and the perturbed gravitational potential by ϕ_g , these three equations are, in the case of a pressureless gravitating fluid (Peebles 1980; Gramann 1993), the mass continuity equation,

$$\frac{\partial \delta}{\partial D} + \nabla \cdot \mathbf{v} + \delta \nabla \cdot \mathbf{v} + (\mathbf{v} \cdot \nabla) \delta = 0, \tag{1}$$

the momentum conservation equation,

$$\frac{\partial \delta}{\partial D} + (\mathbf{v} \cdot \nabla)\mathbf{v} + \frac{3\Omega}{2f^2(\Omega)} \frac{(\mathbf{v} + \nabla \phi_g)}{D} = 0, \tag{2}$$

and the Poisson equation,

$$\nabla^2 \phi_g = \frac{\delta}{D}.\tag{3}$$

In these equations, Ω is the cosmological density parameter, H is the Hubble constant, D(t) is the linear growth factor, and $f(\Omega) = \dot{D}/HD \approx \Omega^{0.6}$ (Peebles 1980).

Although these three equations can be solved using a wide range of assumptions, there are three simple approximate solutions that are useful for reconstructing the primordial density fluctuations. The first method uses the linear perturbation theory approximation, while the remaining two methods use the Zel'dovich approximation together with the assumption that the velocity field remains irrotational during gravitational evolution. We describe these three methods below.

2.1. Linear theory

In linear perturbation theory, which is the simplest approximate solution to the equations listed above, we assume that the density contrast (δ) and the peculiar velocities (v) are small. We can then neglect all the terms involving $\delta \mathbf{v}$ and v^2 . The mass continuity equation can then be trivially integrated over the linear growth factor to give

$$\delta = -D\left(\nabla \cdot \mathbf{v}\right). \tag{4}$$

In this approximation, all the density fluctuations grow at the same rate, and the gravitational potential ϕ_g remains constant throughout the gravitational evolution. If we Fourier transform both sides of equation (4), we see that all the Fourier modes of the density field evolve at the same rate, proportional to D(t), and that the different Fourier modes evolve independently of each other. Further, by combining equation (4) with equation (3), we see that $\phi_g = \phi_v$, where the velocity potential ϕ_v is defined by $\mathbf{v} = -\nabla \phi_v$. Thus, equation (4) gives a simple prescription for recovering the initial density field in the linear theory approximation.

2.2. Zel'dovich-Bernoulli method

The linear theory approximation, being purely local, does not specifically account for the displacements of the mass particles during gravitational evolution. An elegant approximation that addresses this issue is the Zel'dovich approximation (Zel'dovich 1970), in which the mass particles are assumed to move in straight lines during gravitational evolution. In this approximation, the Eulerian comoving position $\mathbf{x}(\mathbf{t})$ of a mass particle at any time t is given in terms of its initial Lagrangian position \mathbf{q} by

$$\mathbf{x}(t) = \mathbf{q} + D(t)\Psi(\mathbf{q}). \tag{5}$$

The essential feature of this Zel'dovich approximation is that the displacement of the mass particle from its initial location is assumed to be separable into a product of two functions, one

of which depends only on time [D(t)] and the other only on the initial location $[\Psi(\mathbf{q})]$. Nusser & Dekel (1992) used the Zel'dovich approximation and the Euler momentum conservation equation together with the assumption that the velocity field remains irrotational during gravitational evolution to derive a first order differential equation for the evolution of the velocity potential ϕ_v :

$$\frac{\partial \phi_v}{\partial D} = \frac{1}{2} |\nabla \phi_v|^2. \tag{6}$$

This equation, called the Zel'dovich-Bernoulli equation, can be easily integrated backwards in time from the present epoch to the initial epoch (defined by $D(t_i) = 0$) to derive the initial velocity potential. Since this equation evolves the velocity potential backwards in time, this reconstruction scheme is best suited to recovering the initial density field from the present day peculiar velocity field. However, after studying N-body simulations, Nusser et al. (1991) suggested the use of the following empirical relationship between the velocity field and the density field in the quasi-linear regime of gravitational instability:

$$\nabla \cdot \mathbf{v} = -\left(\frac{\delta}{1 + 0.18\delta}\right). \tag{7}$$

Thus, given the final density field, we can form the velocity divergence field using equation (7) and then compute the final velocity potential ϕ_v from it using the relation

$$\nabla^2 \phi_v = -\nabla \cdot \mathbf{v}.\tag{8}$$

Once we recover the initial velocity potential, we can use the fact that $\phi_g = \phi_v$ in the linear regime and derive the initial density field from ϕ_g using the Poisson equation.

2.3. Zel'dovich-continuity method

Gramann (1993) showed that the initial gravitational potential is more accurately recovered using the Zel'dovich-continuity equation of Nusser et al. (1991), which combines the Zel'dovich approximation with the mass continuity equation. In this case, the time evolution of the gravitational potential is described by the equation

$$\frac{\partial \phi_g}{\partial D} = \frac{1}{2} |\nabla \phi_g|^2 + C_g,\tag{9}$$

where C_g is the solution of the Poisson type equation

$$\nabla^2 C_g = \sum_{i=1}^{i=3} \sum_{j=i+1}^{j=3} \left[\frac{\partial^2 \phi_g}{\partial x_i^2} \frac{\partial^2 \phi_g}{\partial x_j^2} - \left(\frac{\partial^2 \phi_g}{\partial x_i \partial x_j} \right)^2 \right]. \tag{10}$$

The initial gravitational potential can be determined by integrating equation (9) backwards in time to the initial epoch (defined by $D(t_i) = 0$). The initial density fluctuation field can then be derived from this initial gravitational potential using the Poisson equation.

Both the Zel'dovich-Bernoulli and the Zel'dovich-continuity schemes naturally account for the dynamical displacements of the density features during gravitational evolution, albeit in an approximate way. However, equation (6) and equation (9) are both valid only as long as the density fluctuations are in the linear or quasi-linear regimes (defined by $|\delta| \leq 1$). They do not robustly recover the initial density in regions of very high density when the present day structures are highly non-linear ($|\delta| \gg 1$). Therefore, they require that the final density field be smoothed quite heavily to remove any gross non-linearities, before the dynamical evolution equations are integrated backwards in time. We should also note that these two schemes, like linear theory, require a field rather than a distribution of particles or galaxies as their input. In order to generate a grid of values for this field, some sort of mass assignment procedure must be carried out, which necessarily entails a degree of smoothing.

2.4. Gaussianization

The Gaussianization reconstruction method of W92 belongs to the second category of reconstruction schemes. It is based on the assumption, motivated by studying N-body simulations, that non-linear gravitational evolution preserves the rank order of the mass density field. This means that the high density regions in the initial field become the high density regions in the final conditions, low density regions in the initial field become the voids in the final density field, and so on in between. The method employs a monotonic mapping of the smoothed final density field to a smoothed initial mass density field that has a Gaussian one-point distribution function. By construction, this procedure imposes a Gaussian PDF for the initial mass density field. The high overdensities in extreme non-linear regions are mapped to the positive tail of the Gaussian distribution, while the voids are assigned density values in the negative tail (see Figure 3 in W92 for a graphical illustration of the mapping method). The Gaussianization scheme can robustly recover the initial density field even in those places where the present day density field is quite non-linear because it involves a straightforward mapping procedure. Therefore, this method can be used to reconstruct the primordial fluctuations from even mildly smoothed fields. However, this procedure relies on the strong theoretical assumption that the initial density fluctuations have a Gaussian PDF. Moreover, since it maps the smoothed final galaxy density field to a smoothed initial mass density field at the same Eulerian position, it does not explicitly account for any bulk displacements of galaxies during gravitational evolution. These displacements are typically quite small (of the order of a few Mpc) and therefore not fatal to the Gaussianization reconstruction procedure itself, but they do reduce its accuracy.

2.5. Hybrid method

NW98 proposed a hybrid reconstruction scheme that enjoys most of the desirable features of both the dynamical methods of the first category and the Gaussianization method of the second category. When applying this scheme, we first evolve the mass density field backwards in time using a modified implementation of the Zel'dovich-continuity scheme that is described by equation (9). When we integrate the gravitational potential backwards in time, we use a smoother potential for the source term in the right hand side of equation (9). We derive this smoother potential from an extra smoothed final density field and integrate this smoother potential backwards simultaneously with the higher resolution density field. NW98 tested different values of the smoothing length while deriving this smoother potential and found that a Gaussian smoothing of $R_s = 4h^{-1}$ Mpc led to the best recovery of the initial density field, when the final density field is smoothed with a Gaussian filter of radius $R_s = 3h^{-1}$ Mpc. We then Gaussianize this recovered *initial* density field, thereby improving the recovery in the high density regions. NW98 demonstrated that this method recovers the initial density field more accurately and robustly than either the Gaussianization or the dynamical schemes alone.

2.6. *PIZA*

The third category of reconstruction methods comprises the schemes that are based on the least action principle. This approach was pioneered by Peebles (1989, 1990), who reconstructed the trajectories of individual mass particles by minimizing the action integral. The action integral is minimized subject to the constraint that the initial peculiar velocities of the mass particles should vanish. As the number of galaxies becomes very large, a straightforward application of this method to reconstruct the initial fluctuations from galaxy redshift surveys becomes very difficult. In fact, as stated in §1, this reconstruction method has so far only been used to trace the formation history of the Local Supercluster (Shaya, Peebles & Tully 1995). Giavalisco et al. (1993) generalized the Zel'dovich approximation using a series expansion and combined it with the least action principle to derive a parametrization for the orbits of mass particles. Susperregi & Binney (1994) adapted this scheme to a mass density field that is defined on an Eulerian grid and tested it on one and two dimensional Gaussian random fields.

In this paper, we choose to test the Path Interchange Zel'dovich Approximation scheme of CG97. This scheme essentially consists of a means of applying Zel'dovich Approximation dynamics directly to an evolved particle distribution and recovering the initial positions and velocities of particles. The Zel'dovich Approximation being the least action solution when particle paths are straight lines, the PIZA scheme is probably the simplest and easiest to apply of the least action based schemes. It also appears to be one of the most promising of the methods based on its potential applicability to catalogs with a large number of galaxies. The particle-based Zel'dovich Approximation has been shown (e.g., Coles, Melott & Shandarin 1993) to be one of the most accurate and robust dynamical approximations for forward evolution of a density field. CG97 showed that the PIZA scheme has similar accuracy to the forward Zel'dovich Approximation when it comes to predicting particle velocities and displacements. We can therefore hope that it will compare favorably with the other methods in tests of their ability to recover the primordial

density fluctuations.

In order to apply the PIZA algorithm to an evolved density distribution (details are given in CG97), we must have the final positions of particles, as the scheme is Lagrangian. We make use of these, final, boundary conditions, and the initial boundary conditions that the Universe was homogeneous and that the particles started with zero velocity. We therefore choose a uniform arrangement such as a grid for the initial positions of the particles. Our task is now to connect each one of these initial positions to the correct final position. This can be done by using the constraint that the action be a minimum, which in this case reduces (see CG97) to the minimization of the sum total of the squares of the particle displacements (from the initial to final position). We minimize this sum by starting from a random arrangement of paths joining initial and final positions, and interchanging the end points of pairs of paths if the new configuration leads to a reduction in the action. We carry out this procedure on random pairs of paths until a minimum in the action is reached. We then have a solution for the displacements at each initial grid point. The initial density field is then given by equation (4).

The six reconstruction schemes described above are all derived using different approaches and/or assumptions. We now systematically test these different methods by reconstructing the smoothed initial mass density field from the same final mass distribution. This will enable us to directly compare the ability of the different reconstruction schemes to reconstruct the various features of the primordial density fluctuation field. Since we would like to recover the initial density field in as much detail as possible, we will concentrate on reconstructions of the initial density field smoothed with a small Gaussian filter of radius $R_s = 3h^{-1}{\rm Mpc}$. At this level of smoothing, the final mass density field still contains many regions that are quite non-linear. The schemes in the first category are all designed to work only in the quasi-linear regime ($|\delta| \leq 1$) and may fail in the extremely non-linear regions. However, we still test the performance of these schemes at this small smoothing scale so as to understand the nature and magnitude of this potential failure. We will also test the different reconstruction methods on final density fields smoothed with Gaussian filters of progressively larger radii. The PIZA scheme requires the final positions of the mass particles as its input. So, for this scheme alone, we smooth the density field after the reconstruction procedure and before comparing it with the smoothed true initial density field.

3. GENERATION OF THE TEST DENSITY FIELD

We will test the different reconstruction schemes on the density field derived from an N-body simulation, for which we know the true initial density field a priori. We first generate a random density field on a periodic cubical box of side $L_{\text{box}} = 200h^{-1}\text{Mpc}$. We choose random phases for the Fourier components of the density field so that the resulting field is a Gaussian random field.

We use the matter power spectrum form suggested by Efstathiou, Bond & White (1992),

$$P(k) = \frac{Ak}{\left[1 + \left[ak + (bk)^{3/2} + (ck)^2\right]^{\nu}\right]^{2/\nu}},$$
(11)

where $a = (6.4/\Gamma)h^{-1}{\rm Mpc}$, $b = (3.0/\Gamma)h^{-1}{\rm Mpc}$, $c = (1.7/\Gamma)h^{-1}{\rm Mpc}$, $\nu = 1.13$ and A is the normalization of the power spectrum. This two parameter family of power spectra is characterized by the amplitude A and by the shape parameter Γ , which is equal to $\Omega_0 h$ in cold dark matter models with a small baryon density and scale invariant initial density fluctuations. We use $\Gamma = 0.25$, a value that is consistent with the observed clustering properties of different galaxy catalogs (Peacock & Dodds 1994). We normalize the power spectrum so that the rms fluctuation in density in spheres of radius $8h^{-1}{\rm Mpc}$ (σ_8) is unity, in accordance with the value measured from optical galaxy redshift surveys (Davis & Peebles 1983). This rms fluctuation amplitude σ_8 is related to the power spectrum P(k) by

$$\sigma_8^2 = \int_0^\infty 4\pi k^2 P(k) \tilde{W}^2(kR) dk,$$
 (12)

where $\tilde{W}(kR)$ is the Fourier transform of a top hat filter of radius $R = 8h^{-1}$ Mpc.

We evolve this density field forward in time using a particle-mesh (PM) code written by Changbom Park. This code is described and tested in Park (1990). We use 100^3 particles and a 200^3 force mesh in this PM simulation. We start the gravitational evolution from a redshift of z=23 and follow it to z=0 in 46 equal incremental steps of the expansion scale factor a(t). We form the final continuous mass density field by cloud-in-cell (CIC) binning (Hockney & Eastwood 1981) the gravitationally evolved discrete mass distribution onto a 100^3 grid. We use a Fast Fourier Transform (FFT) to smooth this final density field, relying on the fact that the boundary conditions are periodic.

4. COMPARISON OF RECONSTRUCTION SCHEMES

We recover the initial density field from the final simulation density field described above, using all six schemes described in §2. Except for the PIZA scheme, we recover the smoothed initial density fields from the final density fields that are smoothed with Gaussian filters of radii $R_s = 3, 5, 8$ and $10h^{-1}$ Mpc. However, since we would like to accurately recover even the small scale structures in the initial density field, we will primarily focus on the density field recovered with a $3h^{-1}$ Mpc Gaussian smoothing. As there are cases in which there are large differences in the performance of the different schemes at different smoothing scales, we also show the contour plots and point to point comparisons of the density fields recovered with a $10h^{-1}$ Mpc Gaussian smoothing. Since the PIZA scheme requires the final positions of all the mass particles, we recover the initial density field from the final discrete mass distribution and then smooth this recovered initial density field with a Gaussian filter of appropriate radius before comparing it with the true

smoothed initial density field. Hence, unlike the other reconstruction schemes, the performance of the PIZA scheme does not depend on the extent to which the Gaussian smoothing and the gravitational evolution of the density field are commutative.

4.1. Visual appearance

Figure 1 shows the isodensity contours in a slice through the smoothed initial density fields. The density fields are recovered from a final density field that is smoothed with a Gaussian filter of radius $R_s = 3h^{-1}$ Mpc. The slices correspond to the density field in the region $(x1, y1) = (50, 50)h^{-1}$ Mpc to $(x2, y2) = (150, 150)h^{-1}$ Mpc at a z-coordinate of $50h^{-1}$ Mpc. The contour levels range from -2σ to $+2\sigma$ in steps of 0.4σ , where σ is the rms fluctuation of the smoothed density field. The true initial density field is shown in panel (a). Linear theory (panel b) does not account for the non-linear growth of structures at all, so panel (b) appears the same as the final smoothed density field. The peaks in the reconstructed density field are thus higher and the voids are more sparsely populated compared to those in the true initial density field. The Zel'dovich-Bernoulli and the Zel'dovich-continuity schemes (panels c and d) both recover the smoothed initial density field quite well in the moderately dense regions, but they fail drastically near the high density regions and the recovered voids are not as deep as those in the true initial density field. The Gaussianization method (panel e) recovers the initial density field quite robustly even near the high density peaks. However, although the contour shapes for the Gaussianized density field are similar to that of the true initial density field on large scales, the structures in the Gaussianized density field are slightly shifted from their true locations. This failure to reproduce the correct locations of corresponding structures is not obvious from this contour plot, but it will show up as an increased scatter in the scatter plot of the density fields that we will consider below. The density fields recovered by the hybrid method and the PIZA scheme (panels f and g respectively) are both dynamically accurate and quite robust in the high density regions. We will quantify the superior reconstruction by the hybrid and the PIZA schemes using the cross-correlation coefficient below. We also note here that the structures in the density field recovered by the PIZA scheme appear rather globular and isotropic compared to those in the true density field.

Figure 2 shows the true initial density field and the density fields recovered from a final density field that is smoothed with a Gaussian filter of radius $R_s = 10h^{-1}{\rm Mpc}$. The format of this figure is identical to Figure 1 except that the contour levels range from -2σ to $+2\sigma$ in steps of 0.2σ . At this large smoothing scale, the gravitationally evolved density field is quite smooth, and as σ is much lower (0.42 compared to 1.28 for $3h^{-1}$ Mpc smoothing), there are fewer highly non-linear structures. Therefore, the dynamical schemes recover the smoothed initial field quite well even in the relatively high density regions. Linear theory is again the most inaccurate scheme, with the shallowness of the voids being particularly noticeable. We will show below that the hybrid and the PIZA schemes still yield the most accurate recovery, although this superior performance

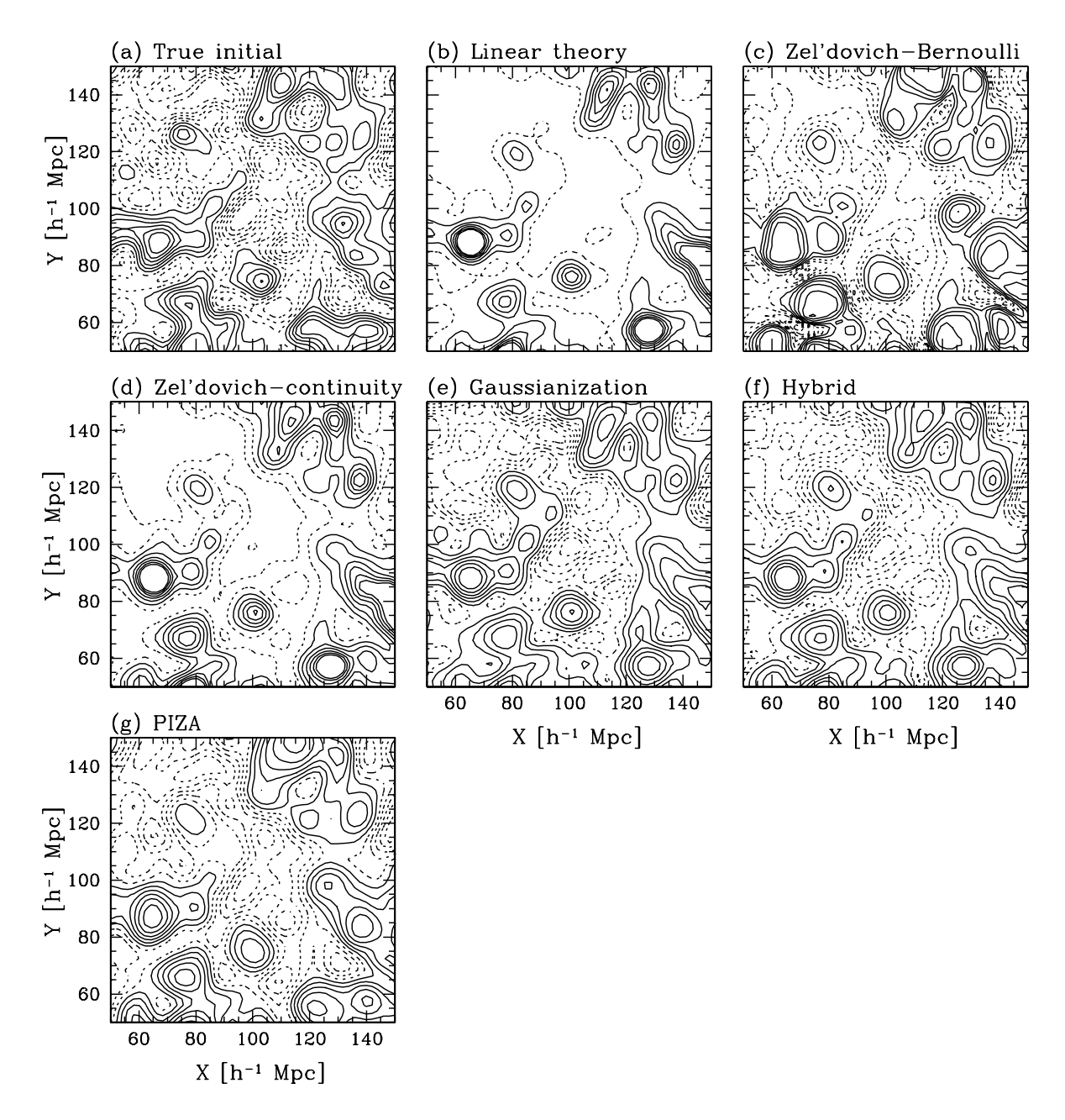


Fig. 1.— Contours in a slice through the true and the reconstructed initial density fields. The density fields are smoothed with a Gaussian filter of radius $R_s = 3h^{-1}{\rm Mpc}$. The contour levels range from -2σ to $+2\sigma$ in steps of 0.4σ . Solid contours correspond to overdensities, while dashed contours correspond to underdensities. (a) True initial conditions, a Gaussian random field with a $\Gamma = 0.25$ power spectrum. Remaining panels show the initial density field reconstructed from the final evolved density field by (b) Linear theory, (c) the Zel'dovich-Bernoulli scheme, (d) the Zel'dovich-continuity scheme, (e) Gaussianization, (f) the hybrid method and (g) PIZA.

is not quite as evident from the contour plots.

4.2. Point-by-point comparison

Figure 3 shows plots of the scatter in a point-by-point comparison of the true and the reconstructed initial density fields in 15625 cells. We plot the density contrast at cells in the reconstructed field (δ_r) against the true initial density contrast (δ_i) at the same cells. Each distribution has been scaled by its RMS value so that the points in a perfect reconstruction lie on a straight line of unit slope. We quantify the accuracy of the reconstruction by the correlation coefficient r between the reconstructed and the true initial density fields,

$$r = \frac{\langle \delta_r \delta_i \rangle}{\langle \delta_r^2 \rangle^{\frac{1}{2}} \langle \delta_i^2 \rangle^{\frac{1}{2}}}.$$
 (13)

Linear theory yields the worst reconstruction of all the schemes. The recovered initial density field does not have any low density regions at all (with $\delta < -1$), and there is a large scatter in the high density regions. The Zel'dovich-Bernoulli scheme recovers the initial densities quite well, with no systematic failures in the quasi-linear regions (characterized by $|\delta| \leq 1$). However, the relation exhibits noticeable curvature in the extremely overdense or underdense regions ($|\delta/\sigma| \geq 2$). The Zel'dovich-continuity scheme also clearly fails in the regions of large density contrasts. It systematically overestimates the initial density in these regions and produces a large scatter, resulting in a weaker correlation. The Gaussianization scheme recovers the initial density field in the highly non-linear regions without any systematic failures. However, its failure to account for the bulk displacements of the mass elements during gravitational evolution leads to a large scatter about the perfect reconstruction $[(\delta/\sigma)_r = (\delta/\sigma)_i]$ and, consequently, a weak correlation. The hybrid scheme corrects for these dynamical displacements using the Zel'dovich-continuity scheme, leading to a tighter correlation between the reconstructed and the initial density fields. The PIZA scheme recovers the initial density field most accurately, without any systematic failures, and it exhibits the strongest correlation among all the reconstruction methods.

Figure 4 shows the scatter plots for the reconstructions from a final density field that is smoothed with a Gaussian filter of radius $R_s = 10h^{-1}{\rm Mpc}$. When a large smoothing length such as this is used before carrying out the reconstruction, the density contrasts are mostly in the linear and quasi-linear regimes, so that the assumptions that go into formulating the Zel'dovich-Bernoulli and the Zel'dovich-continuity schemes are valid. These schemes do recover the initial density field at this level of smoothing fairly accurately, although some curvature of the type seen in the linear theory plot is also present in the Zel'dovich-continuity results. The Gaussianization scheme does not show any curvature and has a good correlation, and the hybrid reconstruction improves this correlation further by including a correction for the displacements of density structures. The PIZA scheme shows the tightest correlation at this smoothing scale and has a visibly smaller scatter.

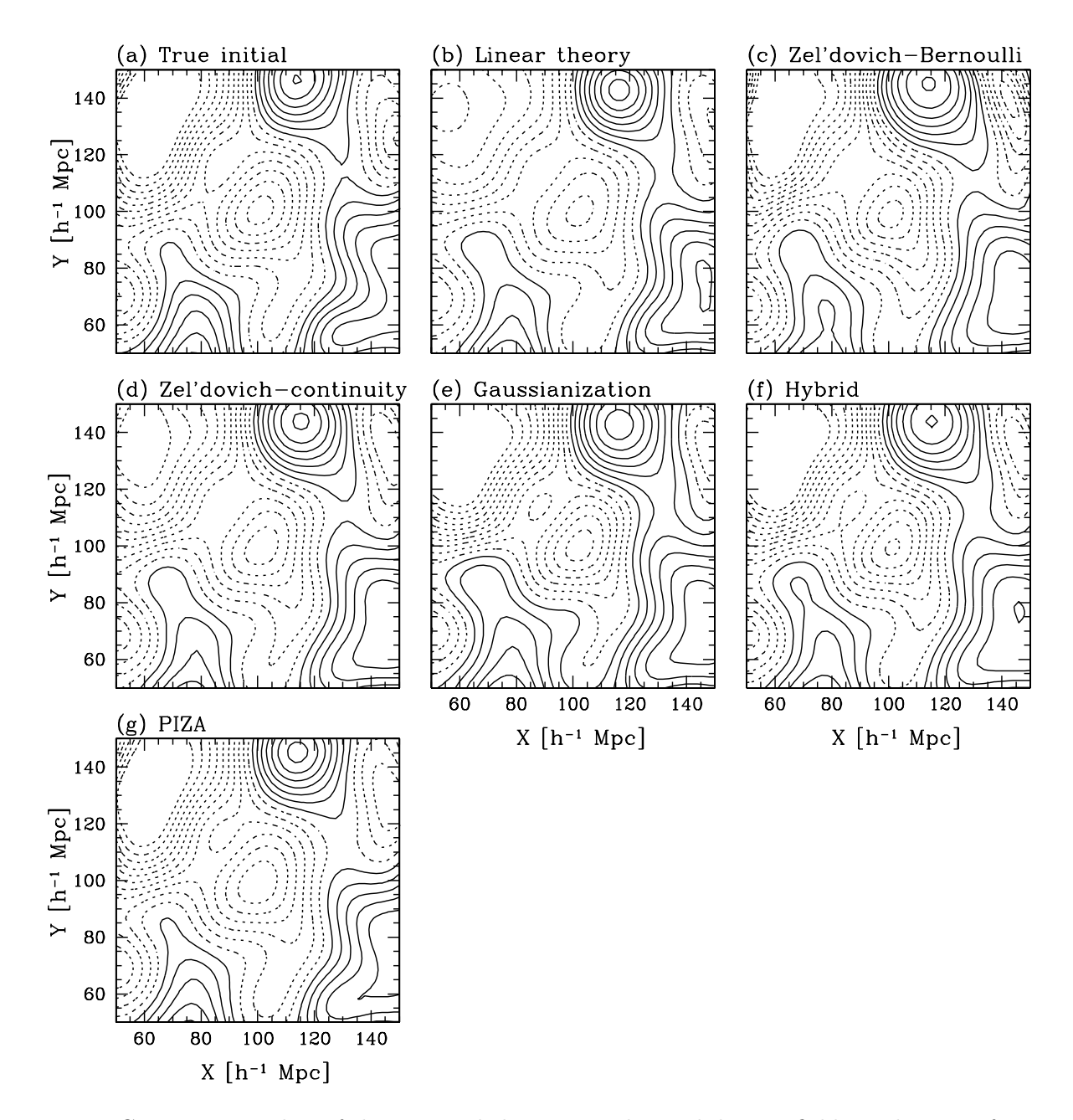


Fig. 2.— Contours in a slice of the true and the recovered initial density fields in the same format as in Figure 1. The density fields are smoothed with a Gaussian filter of radius $R_s = 10h^{-1}{\rm Mpc}$. The contour levels range from -2σ to $+2\sigma$ in steps of 0.2σ .

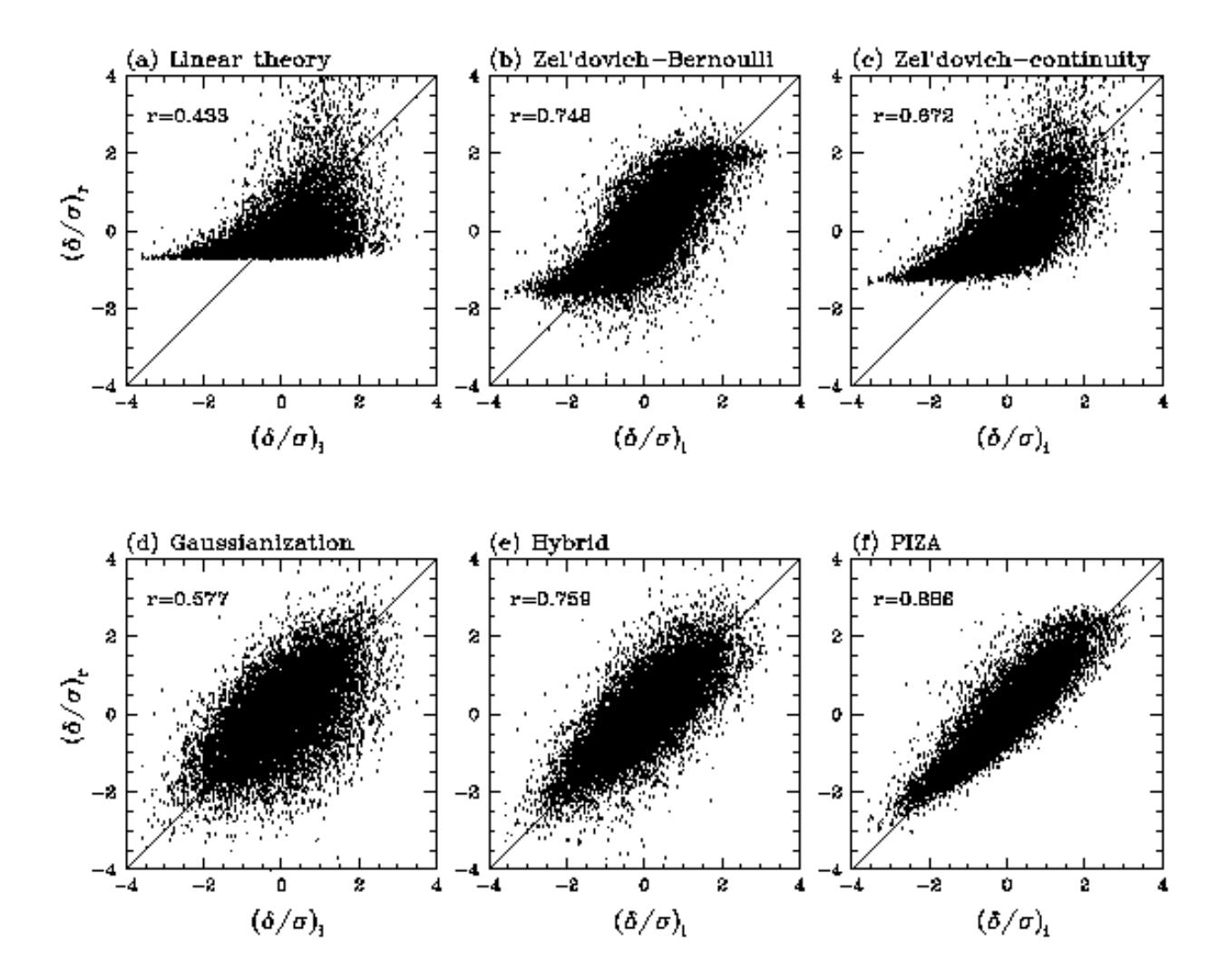


Fig. 3.— Cell by cell comparison of the recovered initial density contrast $(\delta/\sigma)_r$ to the true initial density contrast $(\delta/\sigma)_i$. The density fields are smoothed with a Gaussian filter of radius $R_s = 3h^{-1}$ Mpc. The different panels correspond to the reconstruction using (a) Linear theory, (b) the Zel'dovich-Bernoulli scheme, (c) the Zel'dovich-continuity scheme, (d) Gaussianization, (e) the hybrid method and (f) PIZA. The correlation coefficient between the two fields is indicated in each panel.

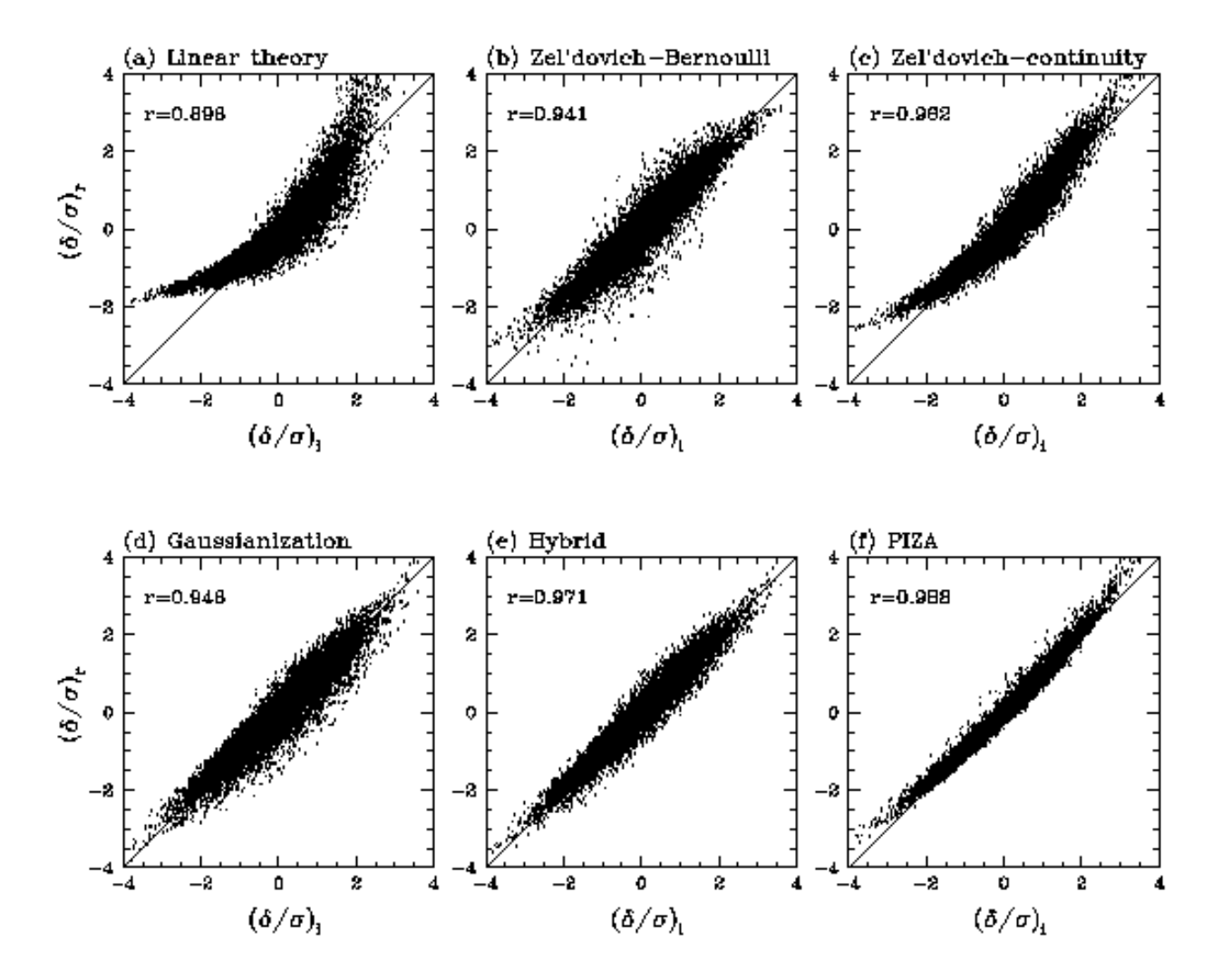


Fig. 4.— Cell by cell comparison of the recovered initial density contrast $(\delta/\sigma)_r$ to the true initial density contrast $(\delta/\sigma)_i$ in the same format as in Figure 3. All the density fields are smoothed with a Gaussian filter of radius $R_s = 10h^{-1}{\rm Mpc}$ and scaled by their rms fluctuation σ .

4.3. Reconstruction performance as a function of smoothing scale

When we reconstruct the initial density fields with a small smoothing filter as in Figures 1 and 3, it is interesting to see how well the information on larger scales is preserved. For example, we have seen that many of the schemes work rather poorly when a point by point comparison is carried out between the reconstructed and true initial fields without any additional smoothing. To reach the results we show next (Figure 5), we have applied additional smoothing to the reconstructed and true initial density fields. Figure 5 shows the correlation coefficient as a function of the effective (total) Gaussian smoothing radius. We first recover the initial density field from a final density field that is smoothed with a Gaussian filter of radius $R_1 = 3h^{-1}$ Mpc. We then smooth this recovered initial field with another Gaussian filter of radius $R_2 = (R_{\text{eff}}^2 - R_1^2)^{1/2}$, so that the recovered density field is smoothed, in effect, with a Gaussian filter of radius R_{eff} . This behavior will help us understand how accurately the information about the initial density field on different scales is recovered by the various reconstruction schemes, when they are used to reconstruct the initial density field smoothed on a particular scale. This plot clearly shows that the PIZA scheme yields the tightest correlation between the true and the recovered initial density fields at all scales. The hybrid scheme and the Zel'dovich-Bernoulli scheme recover the initial density field to almost the same accuracy at the different smoothing scales. The Zel'dovich-continuity scheme is quite poor at recovering the small scale features and becomes progressively better in comparison with the other schemes at larger scales. The Gaussianization scheme shows a weak correlation on all scales because of its inherent Eulerian nature. The linear theory scheme becomes relatively much worse as at the smallest scales.

In Figure 5, we showed how the information about the initial density field on different scales is recovered when it is reconstructed from a final density field that is smoothed with a Gaussian filter of radius $R_s = 3h^{-1}$ Mpc. Alternatively, we can also reconstruct the initial density field on a particular smoothing scale from a final density field that is smoothed on the same scale. This will enable us to quantify how accurately the different reconstruction schemes can recover the initial density field on a particular smoothing scale. For example, the difference between Figures 3 and 4 is the scale on which the final density fields were smoothed before reconstruction. We now extend the comparison shown in these figures to other scales and show the correlation between the true and the recovered initial fields as a function of the scale of smoothing before reconstruction. These results are presented in Figure 6. A comparison between Figures 5 and 6 indicates the extent to which the effects of gravitational evolution and Gaussian smoothing of the fields commute with each other. The two procedures will give identical results for the linear theory and the PIZA reconstruction methods, because the linear theory reconstruction merely involves a scaling of the amplitude of the final density field, while in the PIZA reconstruction scheme, all the smoothings are performed on the recovered *initial* density field. Figure 6 demonstrates the relative performance of the different reconstruction schemes in the linear, quasi-linear and the non-linear regimes. We see that even with heavy smoothing before reconstruction, none of the schemes can match the accuracy of the PIZA scheme. The two grid-based Zel'dovich approximation schemes

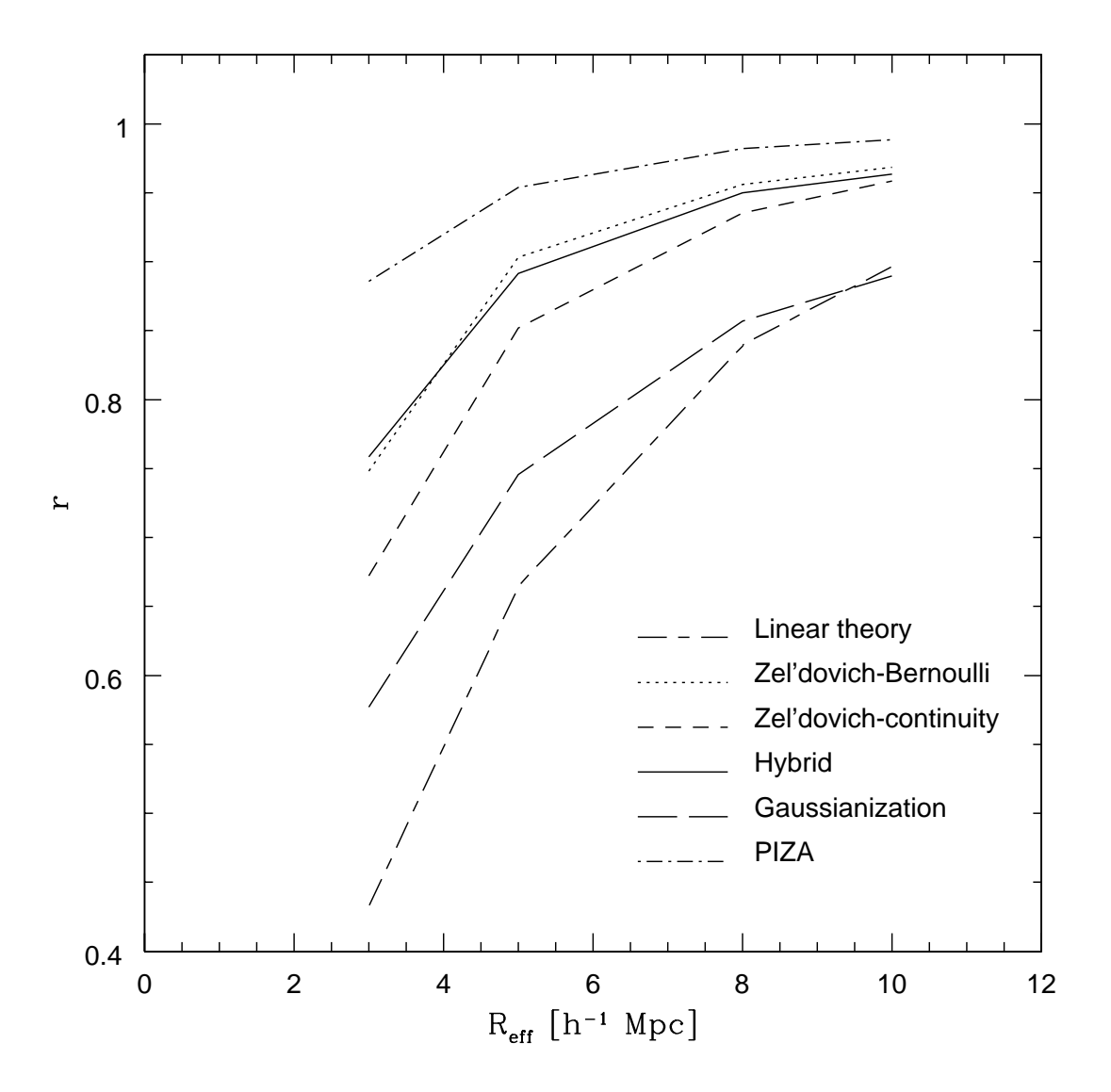


Fig. 5.— Correlation between the true and the reconstructed initial density fields as a function of the effective Gaussian smoothing radius $R_{\rm eff}$, for the various reconstruction schemes. The initial density fields are reconstructed from a final density field that is smoothed with a $3h^{-1}$ Mpc Gaussian filter. The correlation coefficient is calculated after smoothing the recovered initial field further, giving a total effective smoothing $R_{\rm eff}$ (see §4.3).

recover the initial density field with increasing accuracy as we go from the non-linear regime on small scales to the quasi-linear and linear regimes on large scales. We see that at large smoothing lengths the Gaussianization scheme performs almost as well as the Zel'dovich schemes, presumably because the magnitude of the gravitational displacements is now comparable to, or smaller than, the smoothing length of the final density field.

Comparing Figures 5 and 6, we see that the performance of the Zel'dovich-continuity scheme and the hybrid scheme are almost independent of the order of the smoothing and the reconstruction procedures. On the other hand, the performance of the Zel'dovich-Bernoulli and the Gaussianization schemes differs between the two cases. The Gaussianization reconstruction shows a higher correlation at any scale when the *final* density field is smoothed at the same scale. However, the Zel'dovich-Bernoulli scheme shows the opposite behavior, and yields a higher correlation when the *initial* density field recovered from a mildly smoothed final density field is again smoothed using a larger Gaussian filter. This is rather surprising, given that moderate density contrasts are supposedly a requirement of such a quasi-linear treatment. The explanation is probably that the empirical correction (eq. [7]) to the final density field is most effective at relatively small smoothing lengths.

4.4. Phase and amplitude correlations of the recovered fields in Fourier space

A natural measure of the relative accuracies of the reconstructions as a function of scale arises in Fourier space, where we can quantify how well the different Fourier components of the true initial density field are recovered by the different schemes. Figure 7 shows the quantity

$$D(k) = \frac{\sum |\tilde{\delta}_r(\mathbf{k}) - \tilde{\delta}_i(\mathbf{k})|^2}{\sum \left(|\tilde{\delta}_r(\mathbf{k})|^2 + |\tilde{\delta}_i(\mathbf{k})|^2\right)},$$
(14)

where the subscripts i and r refer to the true and the recovered initial density fields respectively. The summation is over all the waves with wavenumbers in the interval $(k - k_f, k]$, where $k_f = 2\pi/L_{\text{box}} = 0.0314 \ h \ \text{Mpc}^{-1}$ is the fundamental wavenumber of the simulation box of side $L_{\text{box}} = 200h^{-1}\text{Mpc}$. This statistic measures the difference in both the amplitudes and the phases of the Fourier components of the true and the recovered initial density fields, and was first used by Little, Weinberg & Park (1991) to demonstrate the effects of power transfer from large scales to small scales during non-linear gravitational evolution. When the complex amplitudes of the Fourier components of the true and the recovered initial density fields are identical, D(k) = 0, while for two fields with uncorrelated phases, the average value of D(k) = 1. This quantity is independent of any smoothing of the density fields after reconstruction and can test the ability of the different schemes to recover the Fourier components even below the smoothing scale. The arrow marked $k_{\rm nl}$ in the Figure shows the wavenumber $k_{\rm nl} = 2\pi/2R_{\rm th} = 0.392 \ h{\rm Mpc}^{-1}$ that corresponds to the top-hat radius $R_{\rm th} = 8h^{-1}{\rm Mpc}$, at which the rms amplitude of density fluctuations is unity in linear theory. This scale can be taken as a boundary between modes in the linear and non-linear

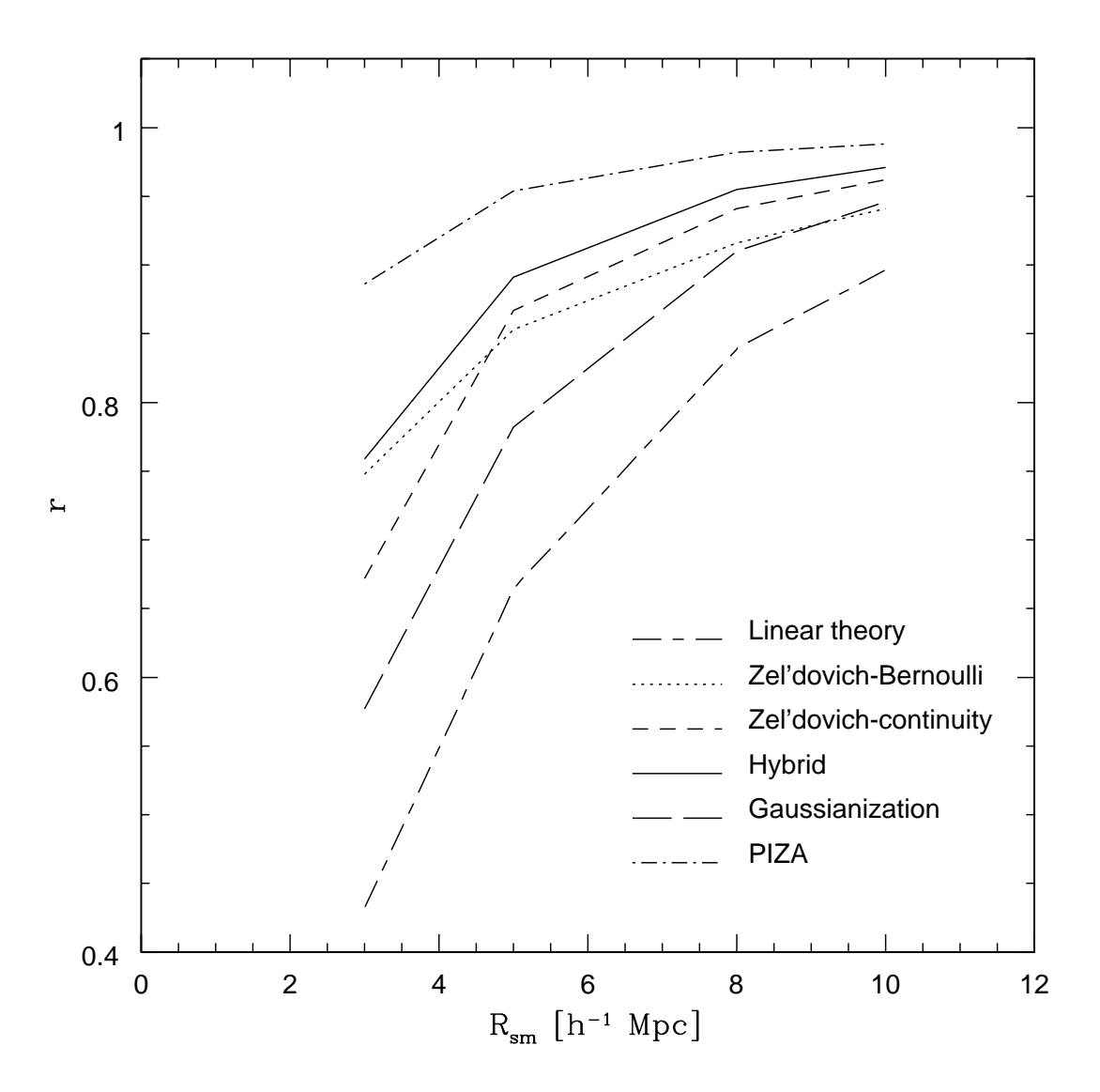


Fig. 6.— Correlation between the true and the reconstructed initial density fields as a function of the radius $R_{\rm sm}$ of the Gaussian filter used to smooth the final density field before reconstruction.

regimes of gravitational evolution. The large scale density modes with $k < k_{\rm nl}$ are still in the linear regime and evolve almost independently of each other, thereby retaining the phase information of the true initial density field. On the other hand, the small scale modes with wavenumbers $k > k_{\rm nl}$ have all experienced phase shifts due to the strong coupling between the evolution of the different modes in the non-linear stages of gravitational evolution (Ryden & Gramann 1991). We find that the PIZA scheme recovers the Fourier modes of the true initial density field most accurately over a wide range of scales. The hybrid and the grid-based Zel'dovich dynamical schemes recover the initial Fourier components quite well up to the non-linear wavenumber $k_{\rm nl}$, but they fail at the larger wavenumbers. The Gaussianization scheme is the only one which fails to recover the true phases for the smallest wavenumbers, giving even worse results than linear theory. This behavior shows that the inaccuracies are not confined to small scales when the reconstruction smoothing scale is so small that the approximation of a monotonic Eulerian transformation between the initial and the final density fields breaks down.

4.5. Probability distribution function

In all the tests of the different reconstruction schemes we have considered so far, we have focused on point-by-point comparisons between the true and the recovered initial density fields. We now test how accurately the different schemes can recover the global statistical properties of the true initial density field, beginning with the one point PDF.

Figure 8 shows the PDF of the initial density field and the density field recovered by the various schemes from a final density field that is smoothed with a Gaussian filter of radius $R_s = 3h^{-1}$ Mpc. The true density field has a Gaussian PDF by construction (solid points), while the Gaussianization and the hybrid reconstruction schemes explicitly impose a Gaussian PDF during the recovery procedure. Non-linear evolution of the density perturbations during the gravitational instability process induces a positive skewness in the PDF because, while the overdensities can grow indefinitely with time, the underdensities cannot become more empty than $\delta = -1$. Linear theory ignores this non-linear evolution and hence does not restore the symmetry of the initial PDF. The Zel'dovich-Bernoulli and the Zel'dovich-continuity schemes are designed to reverse the effects of gravity in the linear and the quasi-linear regimes only. The perturbation expansions on which they are based break down in the very non-linear regions, with the result that they do not fully restore the symmetry between the positive and negative fluctuations of the true initial PDF. The performance of the PIZA reconstruction scheme is impressive, because it derives the initial PDF from the final density field rather than imposing it by assumption. The initial density field recovered from the PIZA scheme does seem to be oversmooth, however, so that there are not enough highly overdense and highly underdense regions. This will have some consequences for the properties of peaks in the density field recovered by PIZA, as we will see below.

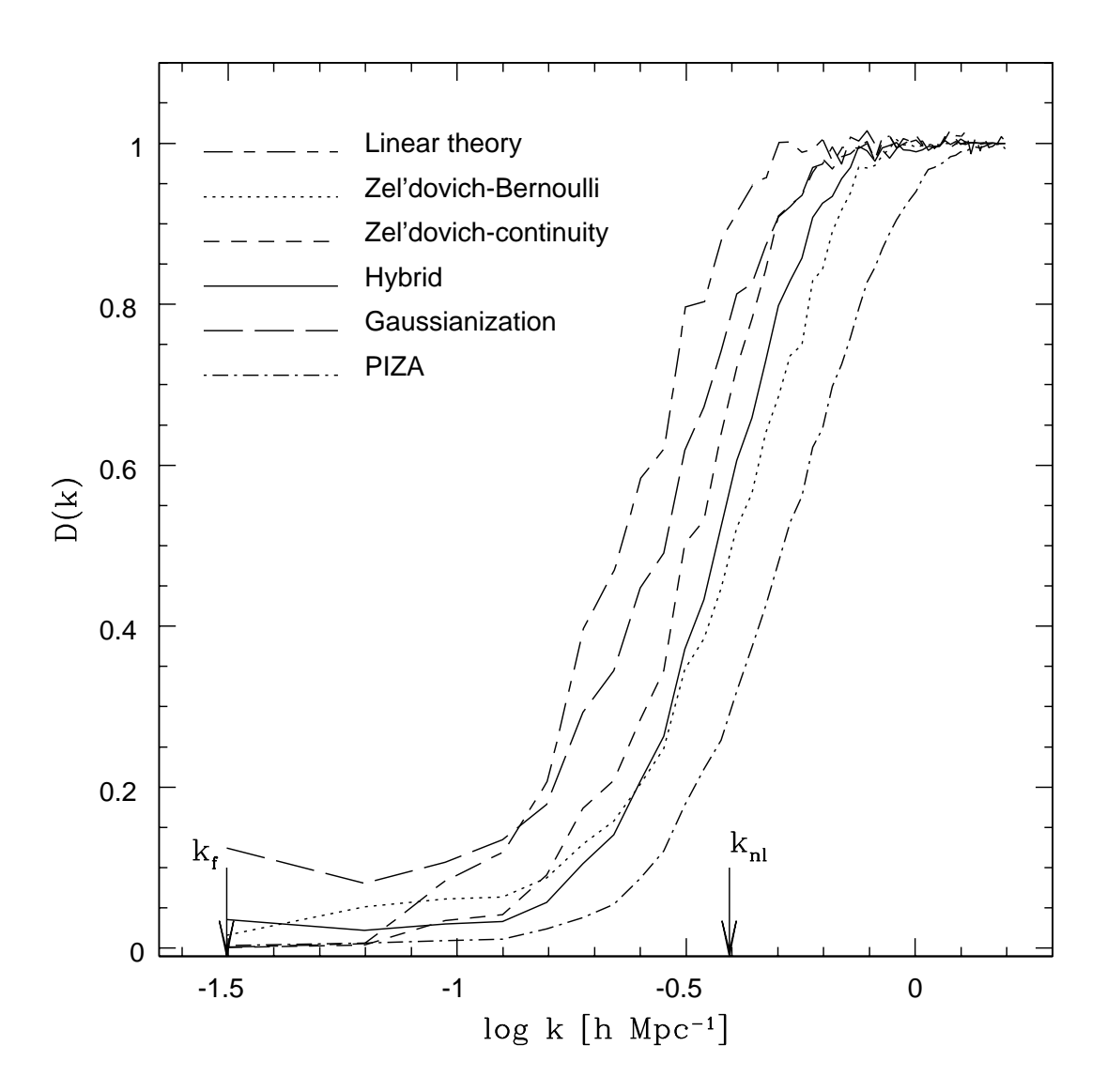


Fig. 7.— Square of the difference between the complex amplitudes of the Fourier components of the true and the recovered initial density fields, divided by the sum of their power spectra (see eq. [14]).

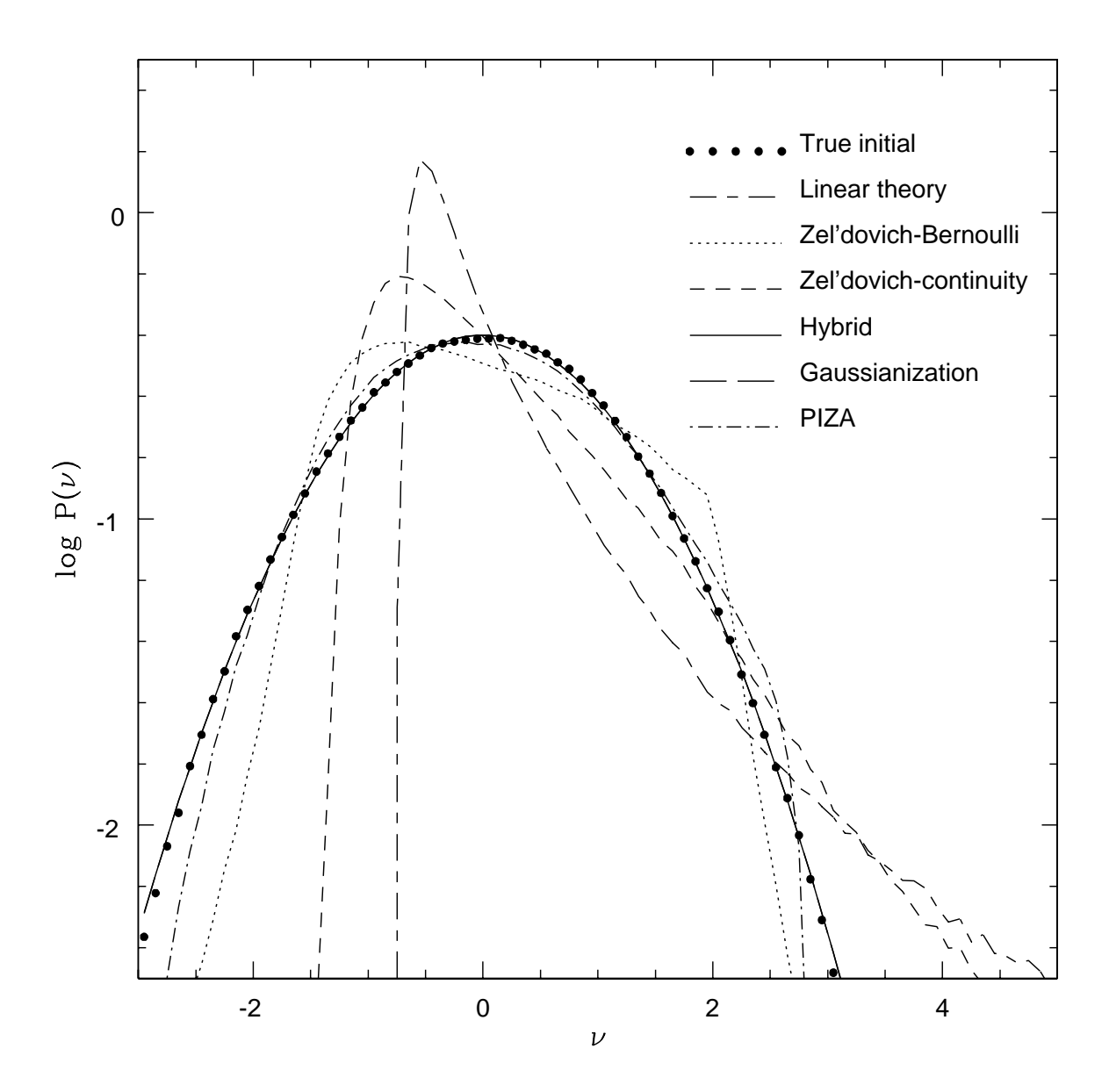


Fig. 8.— PDF of the true initial density field and the density field recovered by the six different reconstruction schemes for a Gaussian smoothing with $R_s = 3h^{-1}$ Mpc. The PDF of the Gaussianization reconstruction is covered by that of the hybrid reconstruction, as both the PDFs are exactly Gaussian by construction.

4.6. Topology

Another global statistic is shown in Figure 9, the genus of the isodensity contour surfaces in the true and the recovered smoothed initial density fields as a function of the contour threshold density ν_V . The genus G_s of a contour surface is defined as (Weinberg, Gott & Melott 1987),

$$G_s = (\text{Number of holes}) - (\text{Number of isolated regions}).$$
 (15)

The contour threshold ν_V is defined implicitly in terms of the fraction (f) of the total volume that is enclosed by this isodensity contour as

$$f = (2\pi)^{-1/2} \int_{\nu_V}^{\infty} e^{-t^2/2} dt.$$
 (16)

For a Gaussian random field, ν_V is equal to the number of standard deviations by which the threshold density differs from the mean density (i.e., $\nu_V = \nu = \delta/\sigma$). The true initial density field (filled circles) has the "W" shaped curve that is characteristic of a Gaussian random field (Doroshkevich 1970; Adler 1981; Bardeen et al. 1986, hereafter BBKS; Hamilton, Gott, & Weinberg 1986). Since Gaussianization preserves the rank order of the pixels, it does not change the topology of the density field. Thus, the genus curves of the density fields recovered using linear theory and the Gaussianization reconstruction schemes are identical, as are the genus curves of the fields reconstructed using the Zel'dovich-continuity scheme and the hybrid method. Mildly non-linear gravitational evolution has only a small effect on the shape of the genus curve, provided that the contour density threshold is defined in terms of the volume enclosed as in equation (16) (Melott, Weinberg & Gott 1988; Park & Gott 1991). The shape of the genus curve of the density field reconstructed by linear theory (which is identical to the genus curve for the Gaussianized field) is therefore very similar to that of the true initial density field, although its amplitude is significantly smaller. This amplitude drop arises due to strong phase correlations in the density field that develop during non-linear gravitational evolution, and it has been observed in numerous studies of the non-linear evolution of the genus curve (Melott, Weinberg & Gott 1988; Park & Gott 1991; Springel et al. 1998). On the other hand, the genus curves for the density fields reconstructed by all the other methods show distinct shifts towards a "meatball" topology (one dominated by isolated clusters).

4.7. Peak heights and shapes

Peaks in the initial density field are potential sites for the formation of galaxy clusters (Kaiser 1984; BBKS; Colberg et al. 1998). They are also the regions that undergo significant non-linear gravitational collapse. We now analyze how accurately the different reconstruction schemes can reproduce the distribution of properties of the peaks in the true smoothed initial density field. Figures 10 and 11 show the number of peaks in the true and the reconstructed initial density fields whose heights are greater than ν times the rms fluctuation σ above the mean density (i.e,

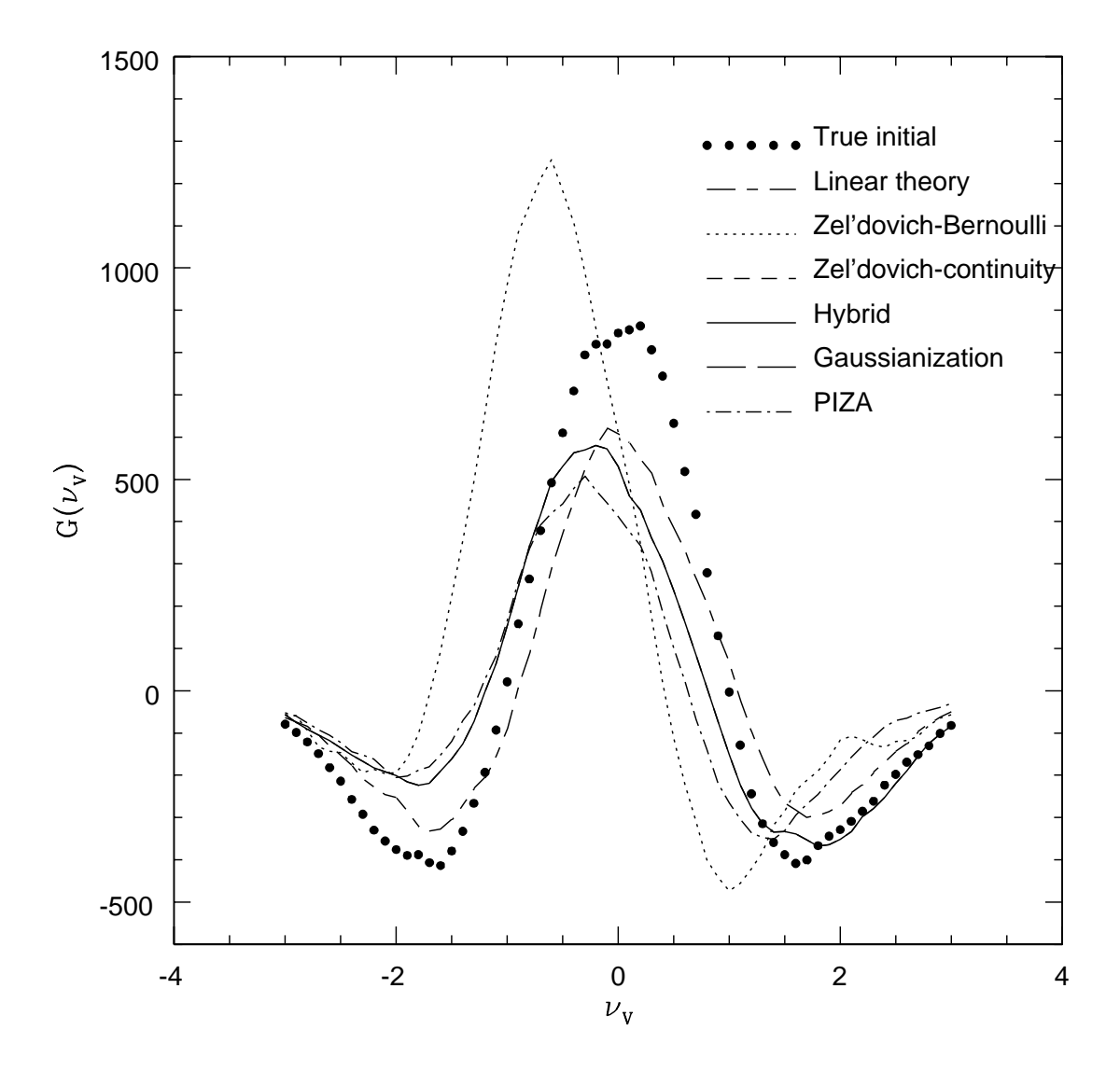


Fig. 9.— Genus curves of the true initial density field and the density field recovered by the different reconstruction methods for a Gaussian smoothing with $R_s = 3h^{-1}$ Mpc. The genus curves of the density field reconstructed using linear theory and the Gaussianization scheme are identical, as are the curves for the density fields recovered using the Zel'dovich-continuity and the hybrid schemes.

 $\nu = \delta/\sigma$). We identify the peaks as those pixels in the density field whose values are higher than all their 26 neighboring pixels. Figure 10 is a linear plot that clearly shows the differences between the different reconstructions for low values of ν , while Figure 11 is a log plot that emphasizes the differences in the high ν region. The filled triangles show this cumulative peak distribution for the true initial density field. The solid circles show the number of peaks of different heights expected in a Gaussian random field of the same volume. We compute this expected number using the equations for the peak number number density in §4 of BBKS. We see that, for $\nu < 2$, there are fewer peaks in the true field compared to the number predicted by BBKS. We find this discrepancy to be due to the coarse resolution used in the CIC binning procedure. The number of peaks for $\nu < 2$ becomes almost equal to the BBKS predicted number if we define the density field on a 200^3 grid instead of on a 100^3 grid. However, all the reconstructed density fields will be affected in the same manner, so we can reliably compare the relative peak distributions of the different reconstructions with respect to that of the true smoothed initial density field.

The Zel'dovich-Bernoulli scheme recovers an excessive number of small and moderately high peaks, but it underestimates the number of very high peaks. From visual inspection, we find that the extra peaks are located near the very high peaks in the true initial density field. This, together with the fact that there is a deficiency in the number of very high peaks, suggests that the extra peaks arise due to the failure of the Zel'dovich-Bernoulli scheme near the highly overdense regions. Thus, a single large peak in the final density field is broken down by the scheme into a large number of moderately high peaks. This is also clear from the large number of ridge-like features surrounding the overdense regions in panel (c) of Figure 1. Linear theory and the Zel'dovich-continuity scheme behave in the opposite manner, with an excessive number of very high peaks and a deficiency of moderate height peaks. The Gaussianization and hybrid schemes recover the peak distributions quite well, as a result of their robust performance in the very high density regions. The PIZA scheme, on the other hand, severely underestimates the number of peaks at all values of ν , and there are no peaks whose heights are greater than 3σ above the mean density in the recovered initial density field.

The PDFs of the initial density fields shown in Figure 8 suggest that at least part of the discrepancy in the peak number distribution can arise from differences in the PDFs themselves. To check if the difference is due to some new failure of the reconstruction procedures or merely the consequence of incorrect PDFs, we compare the peak number distribution after imposing a common PDF on all the reconstructed initial density fields. We Gaussianize the initial density fields recovered by all the reconstruction methods other than the Gaussianization and the hybrid schemes. Figure 12 shows the peak number distribution after all the density fields have been given the same Gaussian PDF. The resulting density field for the linear theory reconstruction will be identical to the density field reconstructed by Gaussianization, while the results for the Zel'dovich-continuity scheme will be identical to those for the hybrid reconstructed density field. Therefore, we do not show the peak number distribution for these two reconstructions in this Figure. The Zel'dovich-Bernoulli reconstruction now agrees well with the true initial peak number

distribution, suggesting that the discrepancy seen in Figure 11 is largely due to an erroneous PDF (as shown in Figure 8). The PIZA scheme now matches better with the true peak distribution at the high peak height end, although there is still a large discrepancy for peaks with $\nu < 3$, by as much as a factor of 3. This means that the rounding off of the PDF is probably not the dominant problem affecting the number of peaks in the PIZA scheme. The slightly oversmoothed nature of the recovered density field seen in Figure 1g seems to make a number of smaller peaks disappear altogether.

An obvious feature in the iso-density contour plots of Figure 1 is that the structures in the reconstructed density fields appear more globular and isotropic compared to the corresponding structures in the true initial density field. To investigate this quantitatively, we define a peak anisotropy parameter σ_a to be

$$\sigma_a^2 = \sigma_f^2 + \sigma_e^2 + \sigma_v^2. \tag{17}$$

In the above equation, σ_f , σ_e , and σ_v are the standard deviations in the density values of the pixels that share either a face, an edge, or a vertex with the peak pixel. Figure 13 shows the distribution of the peak anisotropy parameters of all the peaks in the true and the reconstructed initial density fields. We see that the median anisotropies of the peaks in all the reconstructed fields are smaller than that of the true initial density field. The anisotropy distributions of the hybrid and the Gaussianization reconstructions are closest to that of the true initial distribution. Linear theory and the Zel'dovich schemes recover a large tail of highly anisotropic peaks, reinforcing our conclusions from Figure 1 regarding the poor performance of these schemes near the high density regions. The PIZA scheme recovers peaks that are more isotropic compared to the true peaks, and there are no peaks with $\sigma_a > 0.4$. We also calculated this peak anisotropy distribution after imposing a Gaussian PDF on all the reconstructed initial density fields. We found that the distributions changed very little and our conclusions are unaffected by this. We also found the same behavior for peaks above any given threshold value. A plausible reason for this increased isotropy could be that, in the absence of any information about the initial small scale anisotropies in the final density field, which has been erased by non-linear evolution, the reconstruction schemes tend to recover isotropic structures.

5. DISCUSSION

We have tested the accuracy of six different reconstruction schemes, which fall into three general categories, for recovering the smoothed initial density field from a gravitationally evolved mass distribution. We compared their relative performances in an ideal setting in which the density fields are defined in a cubical box with periodic boundary conditions. We recovered the initial density fields smoothed with Gaussian filters of radii $R_s = 3, 5, 8$ and $10h^{-1}$ Mpc. This range of smoothing lengths is representative of the smoothing scales at which the final density field can be reliably constructed from present day galaxy redshift catalogs. Our conclusions regarding the performance of the different reconstruction schemes can be summarized as follows:

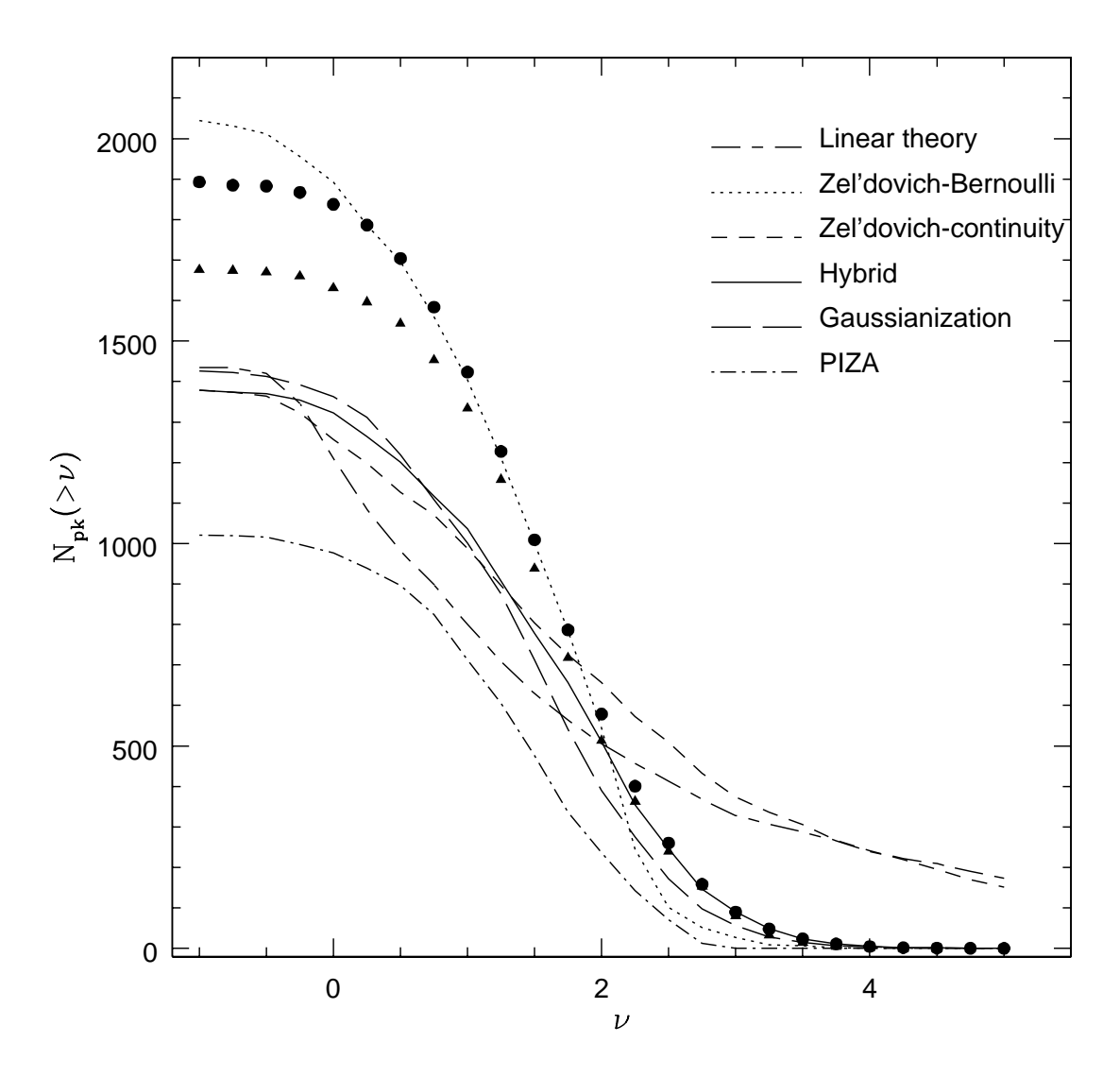


Fig. 10.— Number of peaks in the true and the reconstructed initial density fields whose heights are greater than $\nu\sigma$ above the mean density. The filled circles show the number of peaks predicted by the BBKS formalism, while the filled triangles show the number of peaks present in the true initial density field.

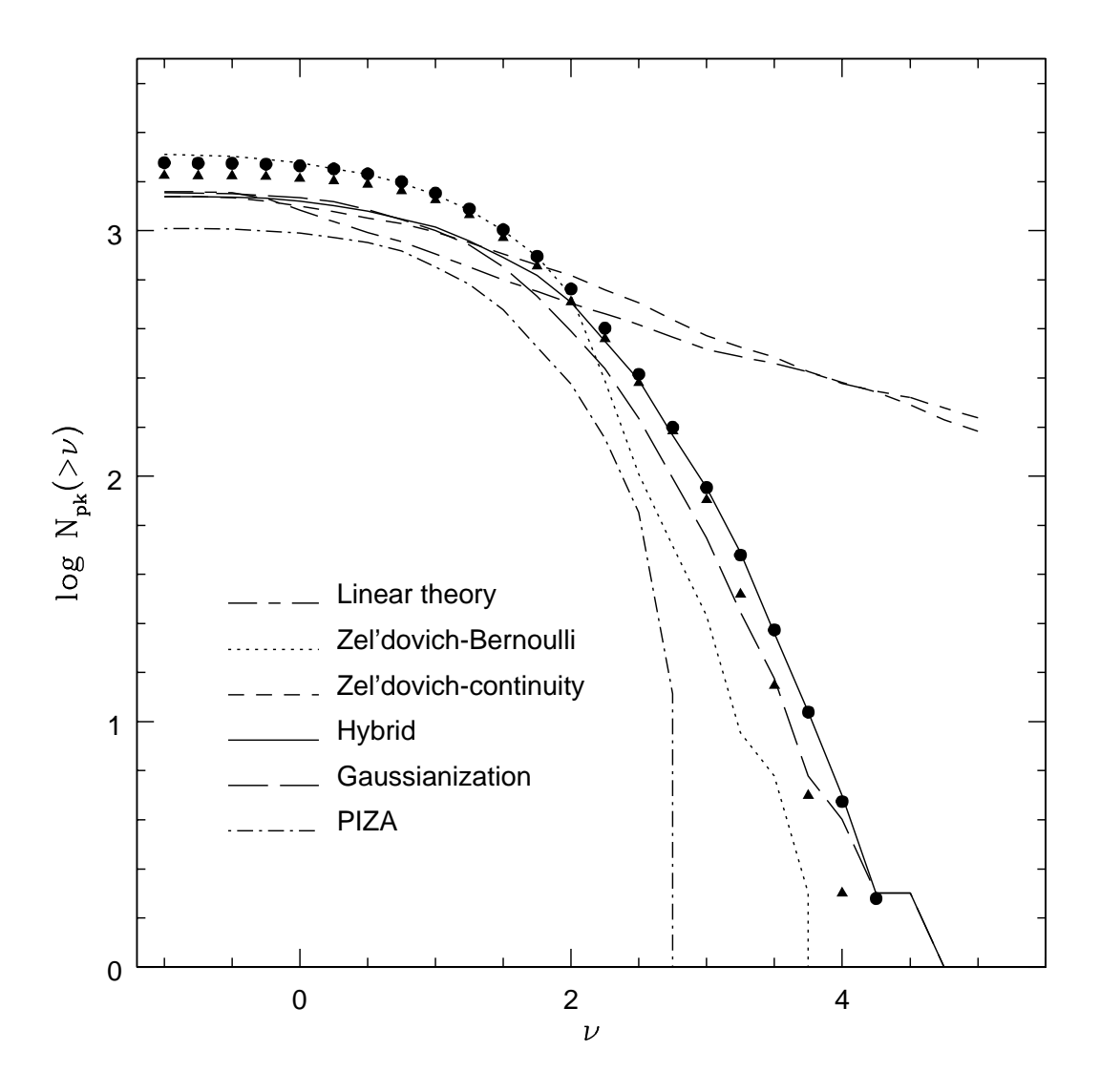


Fig. 11.— Same as Fig. 10, but with a logarithmic scale to emphasize the behavior of high ν peaks.

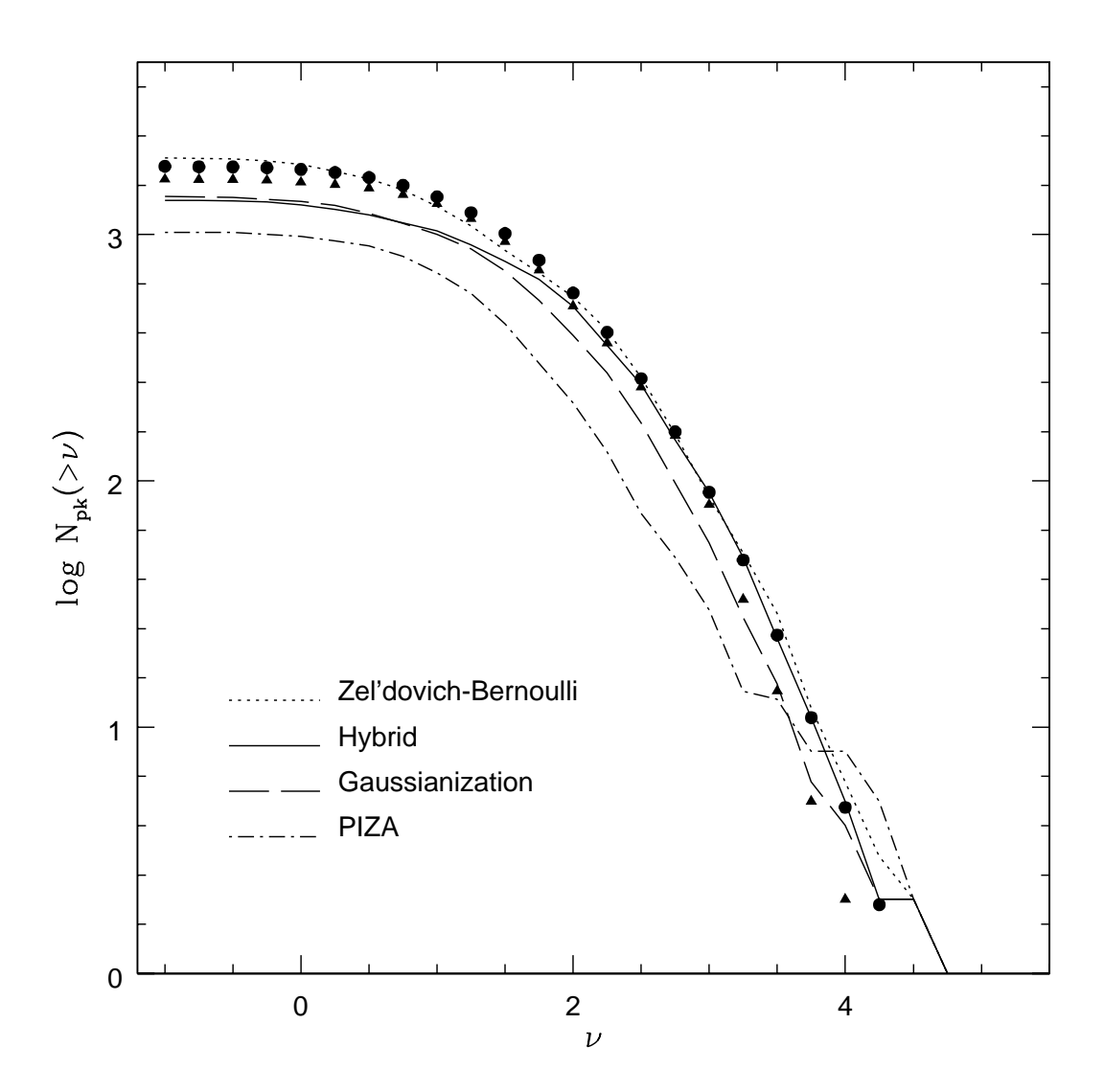


Fig. 12.— Same as Fig. 11, except that the initial density fields recovered by the Zel'dovich-Bernoulli and PIZA schemes have been Gaussianized so that all the density fields shown in this Figure have a Gaussian PDF.

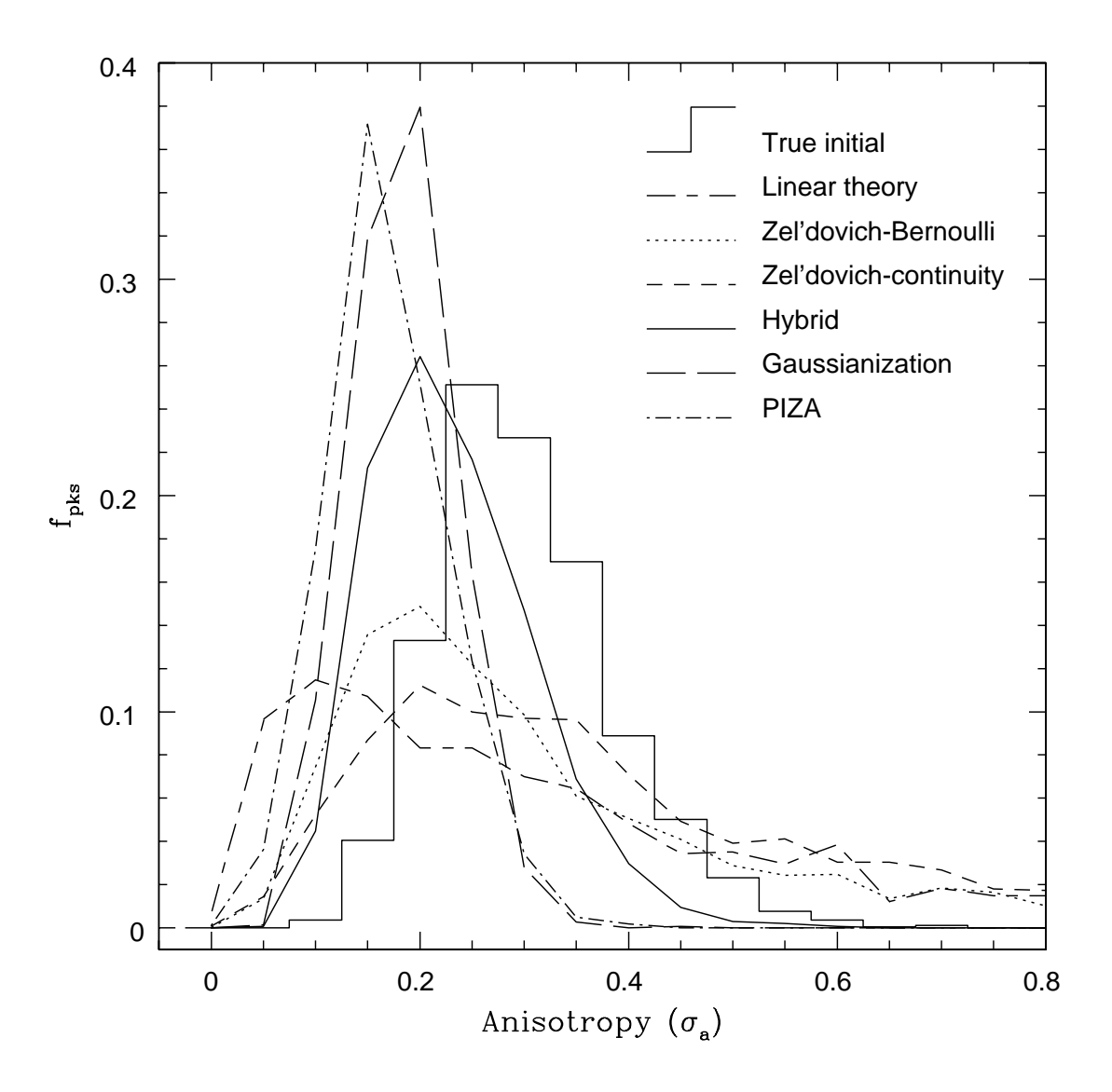


Fig. 13.— Distribution of the peak anisotropies (see equation [17]) in the true and the reconstructed initial density fields.

- (1) The linear theory recovered field is the worst match to the true initial field at all scales. The fact that linear theory is so obviously bad compared to the other schemes is quite encouraging, as it shows that the more sophisticated schemes must be reasonably effective at undoing the effects of non-linear gravitational evolution. It also shows us that there is the potential to gain better quality information by using reconstruction methods rather than applying simple linear theory analyses to observational data.
- (2) The schemes based on the Zel'dovich approximation, namely the Zel'dovich-Bernoulli and the Zel'dovich-continuity schemes, recover the density field quite accurately in the quasi-linear regions, but they fail in the highly overdense regions where the mass distribution is very non-linear. The recovery is generally quite poor for the smallest smoothing scale considered (Gaussian smoothing with $R_s = 3h^{-1}\text{Mpc}$), when the perturbation theory assumptions underlying these schemes break down. However, as expected, these reconstruction schemes become increasingly accurate with larger smoothing, when the final density field is less non-linear. Having said this, the Zel'dovich-Bernoulli scheme does perform unexpectedly well in some tests on small scales (see, e.g., Fig. 3 and Fig. 8). This is presumably due to the empirical correction described by equation (7). The beneficial effects of this correction do not appear to be as great for large smoothings, when the Zel'dovich-continuity scheme becomes relatively more accurate.
- (3) The Gaussianization scheme recovers the initial density field quite robustly but not very accurately at all levels of smoothing.
- (4) The hybrid method recovers the initial field both accurately and robustly. There is no systematic failure even for mildly smoothed fields, and the distribution of peak statistics is recovered quite well.
- (5) The PIZA scheme offers the best recovery of all the reconstruction schemes, at all smoothing scales. It is able to reproduce the true initial density field on a point-by-point basis very well even at the smallest smoothing scales considered in this paper. There is, however, too small a number of peaks in the reconstructed density field, and these recovered peaks also tend to be more isotropic than those in the true field.

All the reconstruction schemes in the first and the second category recover the initial density field from a smoothed final density field that is constructed using the galaxy positions in redshift catalogs. A reconstruction from the final density *field* is quite convenient for dealing with the effects of the selection function, and for applying local transformations to the galaxy density field, which might, for example, include a model for the bias between galaxies and mass. However, in the PIZA scheme, we recover the initial density field using the *locations* of all the mass particles in the final mass distribution and then smooth this recovered initial field with a Gaussian filter before comparing it to the true smoothed initial density field. We now describe a modification of the PIZA scheme that makes it applicable to smoothed final density fields.

Given a smoothed final density field on a grid, we convert it to a particle distribution by placing in each grid cell a number of particles proportional to the density at that cell. The locations of particles within the cell are chosen at random. Since the PIZA scheme can be applied to large numbers of particles, we choose a large enough number of particles that reduces the shot noise to a negligible level (we represent a $3h^{-1}$ Mpc smoothing volume at average density with > 400 particles). We then apply the PIZA procedure to this derived mass distribution, in the usual manner (described in §2.6), and finally smooth this reconstructed initial density field. We compare the smoothed initial density field reconstructed by this method to the true smoothed initial density field. We do not describe the results in detail here but only state our main conclusions. For a $3h^{-1}$ Mpc Gaussian smoothing of the final density field, the statistical tests of §4 show the reconstruction to be only slightly inferior to that of the original PIZA scheme applied to the full mass distribution, and still more accurate than the hybrid reconstruction method. However, the recovered density field is very smooth, and there are fewer peaks compared even to the original PIZA reconstructed density field. There are no peaks above $\nu > 2.5$, and the recovered peaks are all more isotropic than those in the true density field.

In carrying out the tests in this paper, we have assumed that we have complete knowledge of the final real space mass distribution. However, any attempt to recover the primordial density fluctuations in the local universe from galaxy redshift catalogs, using the reconstruction methods we have discussed, will have to contend with three important additional issues: the possibility of bias between the galaxy distribution and the underlying mass distribution, the redshift space distortions arising from the peculiar velocities of galaxies, and the selection function of the survey itself. A detailed examination and testing of solutions to these problems is beyond the scope of this paper. However, we will briefly discuss some ways these effects can be handled.

(1) Galaxy bias. There is convincing evidence that the galaxy distributions selected in the infrared and in the optical have different clustering properties (Lahav, Nemiroff & Piran 1990; Saunders, Rowan-Robinson & Lawrence 1992; Fisher et al. 1994). Hence, it is only reasonable to assume that no one of the galaxy distributions is an unbiased tracer of the underlying mass distribution. When the galaxy distribution is biased with respect to the mass distribution, the observed galaxy number density fluctuations will not directly correspond to the true mass density fluctuations. However, it is reasonable to expect this relationship to be a local one, at least on or above one of the smoothing scales we have tested (for an opposing point of view, see Bower et al. 1993). In this case, some of the different reconstruction schemes could deal with bias between the galaxy and mass distributions. For example, the Gaussianization scheme can recover the initial mass density field from the biased final galaxy density field as long as biased galaxy formation preserves the rank order of the final mass density field. This will be true if there is a local, monotonically increasing functional relationship between the mass and the galaxy density fields. On the other hand, the two dynamical schemes that are based on the Zel'dovich approximation require the final mass density field to compute the final gravitational potential, although the Zel'dovich-Bernoulli scheme can be used to reconstruct the primordial mass fluctuation field from the velocity potential, which can be derived directly from the peculiar velocity surveys (see, e.g., Nusser, Dekel & Yahil 1995). The hybrid scheme can be applied to reconstruct biased galaxy density fields, again assuming local biasing, using the procedure described in NW98. In this, we first map the observed smoothed galaxy density field onto a final PDF of the smoothed underlying mass distribution that is determined empirically assuming a value for the amplitude of mass density fluctuations. This derived mass density field can then be evolved back in time to reconstruct the initial density field. We can, in principle, use this mass density field in the PIZA scheme also, converting it to a particle-based realization as described above.

- (2) Redshift distortions. The second problem stems from the fact that the galaxy distribution in redshift space is a distorted version of the real space galaxy distribution, because of the peculiar velocities of the galaxies (Sargent & Turner 1977; Kaiser 1987). On small scales, the primary distortion is due to the velocity dispersions of clusters, which stretch compact real space clusters into elongated "Finger of God" structures along the radial direction in redshift space. We can reduce this distortion by identifying all the galaxies belonging to a cluster and collapsing them all to the redshift of the cluster. On large scales, coherent bulk inflows into overdense regions and outflows from underdense regions amplify the structures in the density field in redshift space. In the PIZA reconstruction scheme, it is a simple matter to include these redshift distortions self-consistently (see CG97). If the input particle positions are in redshift space, the peculiar velocity component of the particle displacements can be automatically subtracted before computing the action. The PIZA method can therefore be used to recover an estimate of the real space final particle distribution from a redshift space final distribution, as well as an estimate of the initial density field. The other reconstruction schemes require a real space density field as an input, which can be derived from the redshift space distribution using the iterative procedure described in Yahil et al. (1991) and Gramann, Cen & Gott (1994). In this, we first derive a model for the peculiar velocity field from the redshift space density field using the perturbation theory relations between the two fields. We then shift the location of a galaxy so that its redshift is now consistent with the Hubble flow and the peculiar velocity at its new location. We derive a new density field from this corrected galaxy distribution and use it to update our model of the peculiar velocity field. We repeat these steps until the real space locations of the galaxies converge. If the galaxy distribution is biased, we can first map the redshift space galaxy density field to a numerically determined real space mass density PDF before deriving the peculiar velocity field (see §4.1 in NW98 for a stepwise description of this procedure). We must bear in mind that it is necessary to assume a value for Ω in order to carry out any such procedures.
- (3) The selection function. Another problem in the analysis of observational data arises from the decrease in the observed number density of galaxies with increasing distance from the observer in flux limited galaxy redshift surveys. This requires that we smooth the final

density field quite heavily to reduce the effects of shot noise, particularly if we wish to reconstruct over a large volume. We also need to understand the selection function of the survey quite accurately, so that we can weight the galaxies in an optimal fashion, while deriving the final continuous density field. There has been considerable progress of late in deriving optimal estimators for the density field from the redshift survey data (Springel & White 1998 and references therein). In dealing with the selection function, we must also be careful to explicitly take into account the fact that it should be applied to the real space positions of galaxies, in order to avoid the "rocket effect" (Kaiser 1987).

The primary goals for reconstructing the primordial density fluctuation field are twofold. First, we can directly determine the statistical properties of the primordial density fluctuation field, such as, for example, the PDF of the initial density fluctuations (Nusser, Dekel & Yahil 1995). These properties can be used to constrain the theoretical models for the origin of these primordial fluctuations. Secondly, we can evolve the reconstructed initial density field forward in time using N-body methods and compare the evolved mass distribution with the observed galaxy and cluster distributions, thereby leading to constraints on the cosmological parameters and the galaxy formation models (W92; Kolatt et al. 1996; NW98).

All the reconstruction methods that recover the primordial density fluctuations from the density field in some volume require that we have an accurate map of the mass distribution in all the regions that have a significant gravitational effect on the mass distribution within this volume. The reconstruction attempts so far have suffered from the lack of galaxy redshift catalogs that cover such a large, representative region of the universe. However, with the completion of new large redshift surveys such as the PSCZ survey (Saunders et al. 1995) and the ORS survey (ORS, Santiago et al. 1995, 1996), which map the distribution of galaxies over a large solid angle of the sky and to a reasonable depth, it is now becoming increasingly possible to accurately recover the properties of the initial density fluctuation field over a cosmologically interesting volume. We hope that the comparative study of methods we have undertaken in this paper will prove useful both to those undertaking reconstruction analyses of these surveys and to those working on new, even more accurate ways of reversing the effects of gravity.

We thank David Weinberg for his suggestions and guidance. This work was supported by NSF Grant AST-9616822 and NASA Astrophysical Theory Grant NAG5-3111.

REFERENCES

Adler, R. J. 1981, The Geometry of Random Fields (Wiley: New York)

Bardeen, J.M., Steinhardt, P.J., & Turner, M.S., 1983, Phys Rev D, 28, 679

Bardeen, J., Bond, J. R., Kaiser, N., & Szalay, A. 1986, ApJ, 304, 15 (BBKS)

Bower, R. G., Coles, P., Frenk C. S., & White, S. D. M. 1993, ApJ, 405, 403

Chiu, W.A., Ostriker, J.P., & Strauss, M.A., 1998, ApJ, 494, 479

Colberg J. et al. 1998, MNRAS, submitted (astro-ph/9805078)

Coles, P., Melott, A.L., & Shandarin, S.F., 1993, MNRAS, 260, 765

Croft, R.A.C. & Gaztañaga, E., 1997, MNRAS, 285, 793 (CG97)

Davis, M., Peebles, P.J.E., 1983, ApJ, 267, 465

Davis, M., Efstathiou, G., Frenk, C. S., & White, S. D. M. 1985, ApJ, 292, 371

Doroshkevich, A. G. 1970, Astrofisika, 6, 581 [Engl. trans. in 1973, Astrophysics, 6, 320]

Efstathiou, G., Bond, J. R., & White, S. D. M. 1992, MNRAS, 258, 1p

Fisher, K.B., Davis, M., Strauss, M.A., Yahil, A., & Huchra, J.P., 1994, MNRAS, 267, 927

Fosalba, P., 1997, & Gaztañaga, E. MNRAS, submitted (astro-ph/9712095)

Giavalisco, M., Mancinelli, B., Mancinelli, P.J., & Yahil, A., 1993, ApJ, 411, 9

Gramann, M., 1993, ApJ, 405, 449

Gramann, M., Cen, R., Gott, R.J., 1994, ApJ, 425, 382

Gunn, J. E. & Weinberg, D. H. 1995, in Wide Field Spectroscopy and the Distant Universe, eds. S. Maddox & A. Aragón-Salamanca, (Singapore: World Scientific), 3 (astro-ph/9412080)

Guth, A.H. & Pi, S.Y., 1982, Phys Rev Let, 49, 1110

Hamilton, A. J. S., Gott, J. R., & Weinberg, D. H. 1986, ApJ, 309, 1

Hawking, S.W., 1982, Physics Letters, 115, 295

Haynes, M.P. & Giovanelli, R., 1986, ApJ, 306, L55

Heavens, A.J., 1998, MNRAS, submitted (astro-ph/980422)

Hockney, R. W., & Eastwood, J. W. 1981, Computer Simulations Using Particles, (New York: McGraw Hill)

Kaiser, N. 1984, ApJ, 294, L9

Kaiser, N. 1987, MNRAS, 227, 1

Kibble, T.W.B., 1976, J. Phys. A, 9, 1387

Kogut, A., Banday, A.J., Bennett, C.L., Gorski, K.M., Hinshaw, G., Smoot, G.F., Wright, E.L., 1996, ApJ, 464, L29

Kolatt, T., Dekel, A., Ganon, G. & Willick, J.A., 1996, ApJ, 458, 419

Lahav, O., Nemiroff, R.J., Piran, Y., 1990, ApJ, 350, 119

Little, B., Weinberg, D.H, Park, C., 1991, MNRAS, 253, 295

Melott, A.L., Weinberg, D.H., Gott, R.J., 1988, ApJ, 328, 50

Narayanan, V.K. & Weinberg, D.H., 1998, ApJ submitted, (NW98) (astro-ph/9806238)

Nusser, A., Dekel, A., Bertschinger, E., & Blumenthal, G., 1991, ApJ, 379, 6

Nusser, A., Dekel, A. 1992, ApJ, 391, 443

Nusser, A., Dekel, A. & Yahil, A., 1995, ApJ, 449, 439

Park, C., 1990, Ph.D Thesis, Princeton University.

Park, C., & Gott, J. R. 1991, ApJ, 378, 457

Peacock, J.A., Dodds, S.J., 1994, MNRAS, 267, 1020

Peebles, P. J. E. 1980, The Large Scale Structure of the Universe (Princeton: Princeton University Press)

Peebles, P.J.E, 1989, ApJ, 344, L53

Peebles, P.J.E, 1990, ApJ, 362, 1

Protogeros, Z. A. M., & Scherrer, R. J. 1997, MNRAS, 284, 425

Ryden, B., Gramann, M., 1991, ApJ, 383, L33

Santiago, B.X., Strauss, M.A., Lahav, O., Davis, M., Dressler, A., Huchra, J.P., 1995, ApJ, 446, 457

Santiago, B.X., Strauss, M.A., Lahav, O., Davis, M., Dressler, A., Huchra, J.P., 1996, ApJ, 461, 38

Sargent, W. W., & Turner, E. L. 1977, ApJ, 212, L3

Saunders W., Rowan-Robinson, M., Lawrence, A., 1992, MNRAS, 258, 134

Saunders W., Sutherland, W., Efstathiou, G., Tadros, H., 1995, in Wide Field spectroscopy and the distant universe, eds. S.J.Maddox & Aragón-Salamanca, A., (Singapore: World Scientific), p.88

Sathyaprakash, B.S., Sahni, V., Munshi, D., Pogosyan, D. & Melott, A.L., 1995, MNRAS, 275, 463

Shaya, E.J., Peebles, P.J.E., & Tully, R.B., 1995, ApJ, 454, 15

Smoot, G.F et al. 1992, ApJ, 396, L1

Springel, V., White, S.D.M., 1998, MNRAS, in press

Springel, V et al. 1998, MNRAS, in press

Starobinsky, A. A., 1982, Phys Lett B, 117, 175

Susperregi, M. & Binney, J., 1994, MNRAS, 271, 719

Weinberg, D.H., 1992, MNRAS, 254, 315 (W92)

Weinberg, D.H., Gott, R.J., & Melott, A.L., 1987, ApJ, 321, 2

Yahil, A., Strauss, M.A., Davis, M. & Huchra, J.P., 1991, ApJ, 372, 380

Zel'dovich, Ya.B., 1970 A&A, 5, 84

This preprint was prepared with the AAS $\mbox{\sc IAT}_{\mbox{\sc E}}\mbox{\sc X}$ macros v4.0.